JOC The Journal of Organic Chemistry

Article

pubs.acs.org/joc

Method for Estimating S_N1 Rate Constants: Solvolytic Reactivity of Benzoates

Mirela Matić, Bernard Denegri,* and Olga Kronja*

University of Zagreb, Faculty of Pharmacy and Biochemistry, A. Kovačića 1, 10000 Zagreb, Croatia

Supporting Information

ABSTRACT: Nucleofugalities of pentafluorobenzoate (PFB) and 2,4,6-trifluorobenzoate (TFB) leaving groups have been derived from the solvolysis rate constants of X,Y-substituted benzhydryl PFBs and TFBs measured in a series of aqueous solvents, by applying the LFER equation: $\log k = s_f(E_f + N_f)$. The heterolysis rate constants of dianisylmethyl PFB and TFB, and those determined for 10 more dianisylmethyl benzoates in aqueous ethanol, constitute a set of reference benzoates whose experimental $\Delta G^{\ddagger}$ have been correlated with the $\Delta H^{\ddagger}$ (calculated by PCM quantum-chemical method) of the model epoxy ring formation. Because of the excellent correlation (r = 0.997), the method for calculating the nucleofugalities of substituted benzoate LGs have been established, ultimately providing a method for determination of the S_N1 reactivity for any benzoate in a given solvent. Using the $\Delta G^{\ddagger}$ vs $\Delta H^{\ddagger}$ correlation, and taking s_f based on similarity, the nucleofugality parameters for about 70 benzoates have been determined in 90%, 80%, and 70% aqueous ethanol. The calculated intrinsic barriers for substituted benzoate leaving groups show that substrates producing more stabilized LGs proceed over lower intrinsic barriers. Substituents on the phenyl ring affect the solvolysis rate of benzhydryl benzoates by both field and inductive effects.

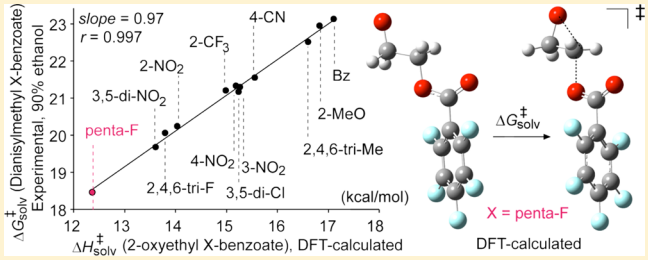

INTRODUCTION

A universally valid nucleofugality scale does not exist because the leaving group ability depends not only on the reaction mechanism but also on various variables such as different solvation effects in various solvents in ground and transition states,[1] back strain effects,[2] anomeric effect,[3] etc. However, a comprehensive empirical scale in which nucleofugalities are defined for combinations of leaving groups and solvents has been developed, based on solvolysis rates of benzhydryl derivatives.[4,5] The nucleofugalities of numerous leaving groups in given solvents have already been added to this scale.[6] According to that approach, the absolute heterolysis rate constant for any S_N1 solvolysis reaction can be expressed with the following three-parameter linear free energy relationship (LFER) equation:

$$\log k = s_f(E_f + N_f) \quad (1)$$

in which k is the first-order rate constant (s^{-1}) at 25 °C, s_f is the nucleofuge-specific slope parameter, N_f is the nucleofugality parameter, and E_f is the electrofugality parameter. Nucleofugality and electrofugality are kinetic terms describing the abilities of the leaving groups to depart with and without the nonbonding electron pair, respectively. E_f is set up as a solvent-independent variable that refers to the ability of the substrate moiety to leave as a carbocation in a heterolysis reaction (S_N1). The nucleofuge-specific parameters (s_f and N_f) describe the leaving group ability in a given solvent. Such an approach separates the contributions of an electrofuge and a nucleofuge in the overall solvolytic reactivity. Predefined parameters are E_f = 0.00 for a dianisylcarbenium electrofuge (X = Y = 4-OCH_3) and s_f = 1.00 for a chloride nucleofuge in pure ethanol. According to eq 1, the nucleofugality (N_f) of a given leaving group is defined as the negative intercept on the abscissa of the log k vs E_f correlation line. This approach enables the estimation of the absolute rates of heterolysis reactions (S_N1) semiquantitatively for various combinations of electrofuge—nucleofuge.[4]

In this work we have focused our attention toward S_N1 solvolysis reactions of fluorinated benzoates, as well as toward benzoates in general, in which the rate-determining heterolysis step involves cleavage of the R—OC(O)Ar bond, and formation of the benzhydrylium carbocation intermediate and the benzoate ion (Scheme 1). Nucleofugalities of the series of substituted benzoates are determined both experimentally and by using quantum-chemical calculation, and the influences of

Scheme 1

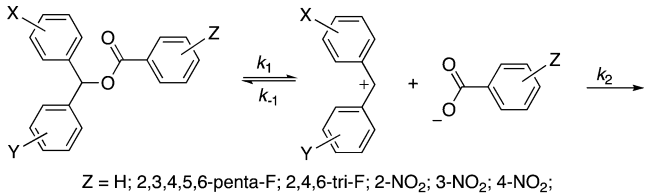

Z = H; 2,3,4,5,6-penta-F; 2,4,6-tri-F; 2-NO_2; 3-NO_2; 4-NO_2; 3,5-di-NO_2; 4-CN; 2-CF_3; 2-MeO; 3,5-di-Cl; and 2,4,6-tri-Me

Received: July 19, 2012
Published: September 13, 2012

   dx.doi.org/10.1021/jo3013308 | J. Org. Chem. 2012, 77, 8986–8998

Table 1. Solvolysis Rate Constants of X,Y-Substituted Benzhydryl Pentafluorobenzoates and X,Y-Substituted Benzhydryl 2,4,6-Trifluorobenzoates in Various Solvents at 25 °C

			k/s^{-1} [c]	
solvent[a]	substrate (X, Y)	E_f[b]	pentafluorobenzoates (PFB)	trifluorobenzoates (TFB)
100E	**2** (PhO, H)	−3.52	1.87×10^{-5}[d]	
	3 (MeO, H)	−2.09	$(3.16 \pm 0.03) \times 10^{-4}$	2.08×10^{-5}[d]
	4 (MeO, Me)	−1.32	$(2.06 \pm 0.04) \times 10^{-3}$	$(1.20 \pm 0.01) \times 10^{-4}$
	5 (MeO, PhO)	−0.86	$(7.69 \pm 0.04) \times 10^{-3}$	$(4.60 \pm 0.07) \times 10^{-4}$
	6 (MeO, MeO)	0		$(3.97 \pm 0.04) \times 10^{-3}$
90E10W	**1** (Me, H)	−4.63	5.65×10^{-6}[d]	
	2 (PhO, H)	−3.52	$(7.74 \pm 0.08) \times 10^{-5}$	3.60×10^{-6}[d]
	3 (MeO, H)	−2.09	$(1.51 \pm 0.01) \times 10^{-3}$	$(7.63 \pm 0.07) \times 10^{-5}$
	4 (MeO, Me)	−1.32	$(9.21 \pm 0.20) \times 10^{-3}$	$(5.10 \pm 0.04) \times 10^{-4}$
	5 (MeO, PhO)	−0.86	$(2.95 \pm 0.07) \times 10^{-2}$	$(1.77 \pm 0.01) \times 10^{-3}$
	6 (MeO, MeO)	0		$(1.25 \pm 0.02) \times 10^{-2}$
80E20W	**1** (Me, H)	−4.63	1.60×10^{-5}[d]	
	2 (PhO, H)	−3.52	$(1.69 \pm 0.03) \times 10^{-4}$	7.92×10^{-6}[d]
	3 (MeO, H)	−2.09	$(3.08 \pm 0.05) \times 10^{-3}$	$(1.55 \pm 0.02) \times 10^{-4}$
	4 (MeO, Me)	−1.32	$(1.70 \pm 0.02) \times 10^{-2}$	$(9.49 \pm 0.10) \times 10^{-4}$
	5 (MeO, PhO)	−0.86	$(3.93 \pm 0.09) \times 10^{-2}$	$(3.04 \pm 0.05) \times 10^{-3}$
	6 (MeO, MeO)	0		$(2.06 \pm 0.02) \times 10^{-2}$
70E30W	**1** (Me, H)	−4.63	$(2.86 \pm 0.01) \times 10^{-5}$	
	2 (PhO, H)	−3.52	$(2.71 \pm 0.10) \times 10^{-4}$	1.39×10^{-5}[d]
	3 (MeO, H)	−2.09	$(4.71 \pm 0.10) \times 10^{-3}$	$(2.52 \pm 0.06) \times 10^{-4}$
	4 (MeO, Me)	−1.32	$(2.21 \pm 0.07) \times 10^{-2}$	$(1.48 \pm 0.01) \times 10^{-3}$
	5 (MeO, PhO)	−0.86		$(3.91 \pm 0.02) \times 10^{-3}$
	6 (MeO, MeO)	0		$(2.86 \pm 0.03) \times 10^{-2}$
90A10W	**3** (MeO, H)	−2.09	$(4.58 \pm 0.02) \times 10^{-5}$	
	4 (MeO, Me)	−1.32	$(2.58 \pm 0.02) \times 10^{-4}$	6.89×10^{-6}[d]
	5 (MeO, PhO)	−0.86	$(8.64 \pm 0.04) \times 10^{-4}$	$(2.72 \pm 0.05) \times 10^{-5}$
	6 (MeO, MeO)	0	$(7.23 \pm 0.06) \times 10^{-3}$	$(2.29 \pm 0.04) \times 10^{-4}$
80A20W	**3** (MeO, H)	−2.09	$(1.59 \pm 0.01) \times 10^{-4}$	
	4 (MeO, Me)	−1.32	$(9.45 \pm 0.05) \times 10^{-4}$	$(3.70 \pm 0.04) \times 10^{-5}$
	5 (MeO, PhO)	−0.86	$(2.88 \pm 0.01) \times 10^{-3}$	$(1.13 \pm 0.02) \times 10^{-4}$
	6 (MeO, MeO)	0	$(2.32 \pm 0.03) \times 10^{-2}$	$(9.76 \pm 0.07) \times 10^{-4}$
70A30W	**2** (PhO, H)	−3.52	1.96×10^{-5}[d]	
	3 (MeO, H)	−2.09	$(4.47 \pm 0.08) \times 10^{-4}$	2.03×10^{-5}[d]
	4 (MeO, Me)	−1.32	$(2.51 \pm 0.04) \times 10^{-3}$	$(1.14 \pm 0.03) \times 10^{-4}$
	5 (MeO, PhO)	−0.86	$(6.64 \pm 0.10) \times 10^{-3}$	$(3.19 \pm 0.03) \times 10^{-4}$
	6 (MeO, MeO)	0	$(4.55 \pm 0.10) \times 10^{-2}$	$(2.55 \pm 0.04) \times 10^{-3}$
60A40W	**2** (PhO, H)	−3.52	$(4.91 \pm 0.02) \times 10^{-5}$	
	3 (MeO, H)	−2.09	$(1.10 \pm 0.01) \times 10^{-3}$	$(5.96 \pm 0.03) \times 10^{-5}$
	4 (MeO, Me)	−1.32	$(5.70 \pm 0.05) \times 10^{-3}$	$(3.32 \pm 0.04) \times 10^{-4}$
	5 (MeO, PhO)	−0.86	$(1.30 \pm 0.02) \times 10^{-2}$	$(8.30 \pm 0.10) \times 10^{-4}$
	6 (MeO, MeO)	0		$(6.33 \pm 0.06) \times 10^{-3}$

[a]Binary solvents are on a volume−volume basis at 25 °C. A = acetone, E = ethanol, W = water. [b]Electrofugality parameters were taken from ref 4. [c]Average rate constants from at least three runs performed at 25 °C unless otherwise noted. Errors shown are biased standard deviations. [d]Extrapolated from data at higher temperatures by using the Eyring equation.

the aromatic ring substitution on overall barriers and intrinsic barriers are examined. Furthermore, a quantum-chemical model is proposed here, whose calculated activation enthalpies correlate very well with experimental activation free energies for solvolysis of the series of dianisylmethyl (X = Y = 4-MeO) benzoates, ultimately enabling the prediction of solvolytic reactivities for a wide spectrum of benzoates with various substituents.

RESULTS AND DISCUSSION

Kinetic Measurements. Equation 1 has been used to assess the reactivity of fluorinated benzoate anions as leaving groups in various solvents and to relate their nucleofugalities to other leaving groups (LG). Benzhydryl derivatives have been employed as substrates, at which the substituents on the benzhydryl moiety have been adjusted to enable kinetic measurements to be carried out by conventional methods. Thus, a series of X,Y-substituted benzhydrylium pentafluorobenzoates (**1-6-PFB**) and 2,4,6- trifluorobenzoates (**2-6-TFB**) have been subjected to kinetic measurements.

A series of benzhydryl pentafluorobenzoates (**1-6-PFB**) and benzhydryl 2,4,6-trifluorobenzoates (**2-6-TFB**) have been prepared from the corresponding benzhydrols according to the methods presented in Experimental Section. The solvolysis rates have been measured conductometrically in various solvents at 25 °C. In a few cases the rates have been measured

dx.doi.org/10.1021/jo3013308 | J. Org. Chem. 2012, 77, 8986−8998

at three different temperatures and extrapolated to 25 °C. Details are given in Kinetic Methods (Experimental Section). The first-order rate constants are presented in Table 1.

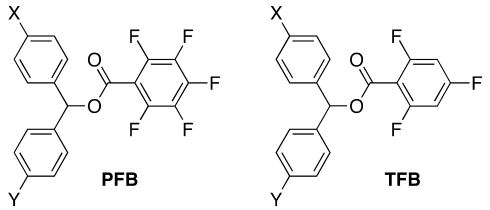

1: X = Me, Y = H
2: X = PhO, Y = H
3: X = MeO, Y = H
4: X = MeO, Y = Me
5: X = MeO, Y = PhO
6: X = MeO, Y = MeO

The nucleofugality parameters (N_f) and the slope parameters (s_f) for PFB and TFB measured in various solvents have been determined according to eq 1 by correlating the logarithms of the first-order rate constants and the corresponding E_f values. Plots of log k against E_f obtained for solvolysis of substituted benzhydryl pentafluorobenzoates in ethanol–water binary solvents are presented in Figure 1 (correlation lines obtained in aqueous acetones and the lines for trifluorobenzoates are shown in Figures S1–S4 of the Supporting Information). The nucleofuge-specific parameters calculated according to eq 1 are presented in Table 2. The nucleofugalities show that the reactivity of TFB is similar to that of DNB,[4] while PFB reacts about 1 order of magnitude faster. Systematically higher reaction constants (s_f) in all solvents for less reactive TFBs than for PFBs confirm that TFB solvolyzes via a later TS in which the charge separation is more advanced. The slope parameters (s_f) decrease for both nucleofuges as the polarity of the solvent increases. Such behavior has been observed earlier and rationalized as diminished solvation of the TS in more polar solvent due to charge dispersion in both nucleofuge and electrofuge moieties.[7,8]

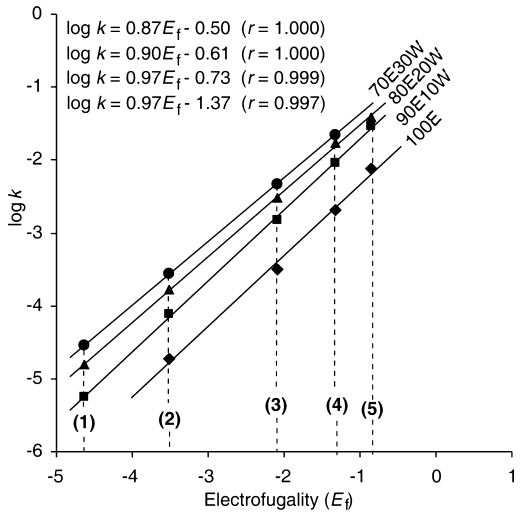

Figure 1. Plots of log k (25 °C) versus E_f for solvolysis of substituted benzhydryl pentafluorobenzoates in ethanol and aqueous solvents of ethanol. Solvent mixtures are given as v/v; E = ethanol and W = water.

At this point of research, experimental reactivities in a series of solvents have been available for five different benzoates, which are as follows: Bz (benzoate), PNB (*p*-nitrobenzoate), DNB (3,5-dinitrobenzoate),[4] and PFB and TFB presented above. Because our intention was to correlate the experimental results with a quantum-chemical model, it was advantageous to expand the range of experimental reactivities that would be correlated. Even more important was to gain experimental data for substrates with structurally versatile leaving groups, those with one or more electron-withdrawing and electron-donating substituents being attached to different positions of the phenyl ring of the benzoate moiety. Reactivities of dianisylmethyl (X = Y = MeO) derivatives have been chosen for correlation, so the rates of seven additional dianisylmethyl benzoates have been determined. To find out the impacts of the enthalpy of activation ($\Delta H^{\ddagger}$) and the entropy of activation ($\Delta S^{\ddagger}$) on the overall reactivity, the solvolysis rates have further been determined at three different temperatures in 90% aq ethanol. The kinetic results are presented in Table S1 (Supporting Information). This expanded set of 12 reference benzoates covers various structures in which electron-accepting groups (NO_2, CN, CF_3) and atoms (F, Cl), as well as electron-donating groups (MeO, Me), are substituents on the phenyl ring of the benzoate moiety. Also, the number of substituents attached to the phenyl ring varies from 0 to 5.

Quantum-Chemical Model for Reference Leaving Group Effects. Nucleofugality has often been associated with the basicity of the leaving groups because a good linear correlation between the reactivity of LGs (log k) and the pK_a values of the conjugated acids of the LGs has been obtained for some substrates. The heterolysis barrier height in solvolysis is defined by two factors: the intrinsic barrier (Λ) and the change in free energy ($\Delta G°$). It is not surprising that numerous

Table 2. Nucleofugality Parameters N_f and s_f for Pentafluorobenzoate (PFB) and 2,4,6-Trifluorobenzoate (TFB) in Various Solvents

	PFB		TFB	
solvent[a]	N_f[b]	s_f[b]	N_f[b]	s_f[b]
100E	−1.41 ± 0.19	0.97 ± 0.05	−2.19 ± 0.10	1.10 ± 0.03
90E10W	−0.76 ± 0.06	0.97 ± 0.02	−1.90 ± 0.08	1.01 ± 0.02
80E20W	−0.68 ± 0.03	0.90 ± 0.01	−1.75 ± 0.07	0.98 ± 0.02
70E30W	−0.58 ± 0.01	0.87 ± 0.01	−1.68 ± 0.06	0.94 ± 0.02
90A10W	−2.04 ± 0.07	1.06 ± 0.02	−3.18 ± 0.19	1.17 ± 0.06
80A20W	−1.58 ± 0.02	1.04 ± 0.01	−2.80 ± 0.01	1.08 ± 0.01
70A30W	−1.41 ± 0.01	0.96 ± 0.01	−2.60 ± 0.06	1.00 ± 0.02
60A40W	−1.15 ± 0.07	0.92 ± 0.02	−2.30 ± 0.07	0.97 ± 0.02

[a]Binary solvents are v/v at 25 °C. A = acetone, E = ethanol, W = water. [b]Errors shown are standard errors.

dx.doi.org/10.1021/jo3013308 | J. Org. Chem. 2012, 77, 8986–8998

Scheme 2. Epoxy Ring Formation Model Reaction

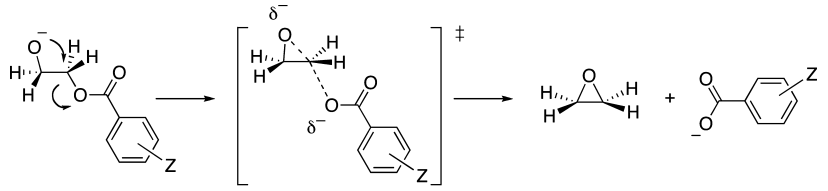

Z = H; 2,3,4,5,6-penta-F; 2,4,6-tri-F; 2-NO_2; 3-NO_2; 4-NO_2; 3,5-di-NO_2; 4-CN; 2-CF_3; 2-MeO; 3,5-di-Cl; and 2,4,6-tri-Me

substrates show deviation from the log k vs pK_a plot, because in such correlations, the intrinsic factor is neglected. Clearly, the solvolytic reactivity of a given substrate cannot be reliably estimated from the basicity of the LG.[9]

To investigate the nucleofugality of numerous substituted benzoate leaving groups, we have searched for a reliable theoretical model, whose reaction barriers obtained by quantum-chemical calculations correlate reasonably well with the experimental barriers of the benzhydryl derivatives. The total (electronic) energy in the heterolytic cleavage of the C—LG bond of neutral substrates continuously increases until interaction between the charged LG and the nearest neighboring hydrogen occurs, preventing location and optimization of the transition state for the heterolytic step of the monomolecular substitution. On the other hand, optimized transition states for S_N2 reactions[10] as well as for displacement reactions that proceed via participation of the neighboring group (anchimeric assistance) are presented in the chemical literature.[11,12] Also, a quantum-chemical study has been used to correlate the experimentally determined free energies of activation for combination of benzhydrylium ions with various π-electrophiles and free energies of activation calculated by different theoretical methods.[13] Although considerable systematic deviations of $\Delta G^{\ddagger}_{calc}$ from the experimental values are obtained, the correlations are reasonably good. Furthermore, Aggarwal et al. using the B3LYP method examined the PES for reactions of ammonium, oxonium, phosphonium, and sulfonium ylides with benzaldehyde and suggested that the ability of the leaving group (nucleofugality) had a distinct influence on the rate of the styrene oxide formation in the intramolecular nucleophilic substitution step.[11] They also demonstrated a notable impact of the intrinsic barrier on the ability of neutral leaving groups (OMe_2, SMe_2, NMe_3, and PMe_3) in the heterolytic step.

We have chosen to compute the epoxy ring formation as a model reaction in which the intramolecular backside n-electron attack of the negatively charged oxygen is a driving force for the C—OCOBz-Z bond cleavage (Scheme 2) and to correlate the activation energies of the model reaction with the experimental barriers of the heterolysis of dianisylmethyl benzoates. Our basic assumption is that the differences in reaction energetics for the series of model reactions are determined mostly from the effects of LGs, while other variables contribute to overall energies similarly (e.g., unfavorable entropy of activation caused by n-electron assistance, solvation effects, etc.)

Quantum-chemical calculations for the model reaction have been performed with various 2-oxyethyl benzoates, and the corresponding transition structures have been optimized. In preliminary calculations the transition-state structures for the oxy-assisted heterolytic cleavage have been optimized in the gas phase with the following leaving groups: PFB, TFB, DNB, PNB, and Bz. Poor correlation has been obtained between the calculated barriers at 25 °C for the epoxy ring formation and the experimental barriers for solvolysis of corresponding dianisylmethyl benzoates (see Figures S11 and S12 in Supporting Information). In addition, due to the anionic form of the substrates, small barriers (ca. 2 to 7 kcal/mol) have been obtained. However, inclusion of the polarizable continuum (water) in optimization increased the barriers and improved the correlation significantly. By applying the PCM model, which mimics the solvent, a different demand for solvation of the ground and the transition state has been taken into account. While the electrostatic solvation of the negative charge located mainly on the oxygen in the ground-state structures is important, the transition structures, in which the negative charge is delocalized, might be less solvated with increasing polarity of medium. The net effect is an increase of the reaction barriers. It should be emphasized that the C—O bond dissociates in all the cases; hence, the impact of hydrogen bonds (electrophilic solvation) on relative reactivity is canceled out and thus inclusion of explicit molecules of solvent in the model reaction is not necessary.

Geometry optimizations, using the Gaussian 09 package,[14] were carried out without any constraints at the B3LYP/6-311+G(2d,p) level. The integral equation formalism model for PCM calculations (IEFPCM) in a dielectric continuum representing water as a solvent has been employed.[15] Details of the calculations are given in Computational Methods below and in Supporting Information (coordinates and energies). The optimized substrate and transition-state structures for the heterolytic epoxy ring formation with 2-oxyethyl 3,5-dinitrobenzoate and 2-oxyethyl 2,4,6-trifluorobenzoate are presented in Figure 2 (other structures are included in Supporting Information).

Lengths of the partial (cleaving) bonds are basically the same in all TS. This is not surprising because the substituents on the benzene ring do not take part in the resonance delocalization of the developing negative charge on the carboxyl group but only electrostatically interact with it. The structures shown indicate that the geometries of the ground and transition states are influenced by the substituents on the phenyl ring. Generally, substituents in the ortho-position cause a substantial twisting of the benzene ring out of the carboxyl group plane, as is shown for 2,4,6-trifluorobenzoate in Figure 2. This twisting effect is more pronounced in the TS, so the dihedral angle between the carboxyl plane and the benzene ring is larger in the TS than that in the ground-state structure in all the cases. Further increase of the dihedral angle in the transition-state structure probably comes from the increase of the spatial electrostatic repulsions between the ortho-substituents and the partially negatively charged carboxyl group. In dynamic systems this might induce the decrease of the rotational degrees of freedom at the transition state, which leads to the decrease of the activation entropy.

dx.doi.org/10.1021/jo3013308 | J. Org. Chem. 2012, 77, 8986−8998

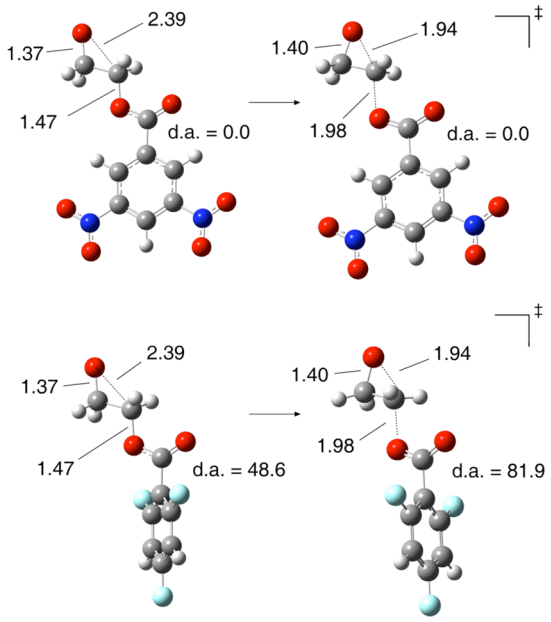

Figure 2. Optimized PCM-B3LYP/6-311+G(2d,p) structures of 2-oxyethyl 3,5-dinitrobenzoate and 2-oxyethyl 2,4,6-trifluorobenzoate and of the related heterolytic transition states. Selected distances are given in angstroms. Dihedral angles (d.a.) between the carboxyl plane and benzene ring are given in degrees.

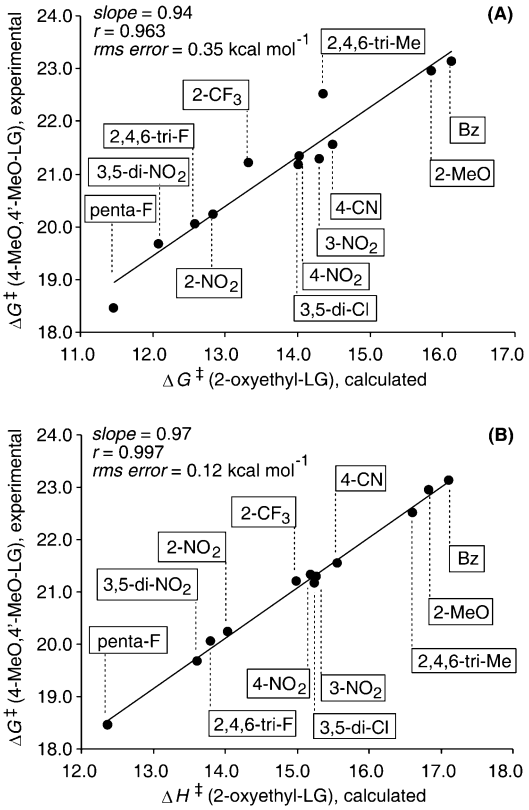

Figure 3. Correlation of experimental activation free energies (kcal mol^{-1}) for solvolyses of dianisylmethyl benzoates in 90% ethanol at 25 °C against PCM-B3LYP/6-311+G(2d,p)-calculated activation free energies (A), and calculated activation enthalpies (B) for heterolyses of 2-oxyethyl benzoates.

Correlation of Experimental and Computed Leaving Group Effects. To compare the leaving group effects on reactivities of the model heterolytic epoxy ring formation (Scheme 2) and of benzhydryl benzoates, we plotted the experimental barriers for solvolysis of 12 reference dianisylmethyl benzoates ($\Delta G^{\ddagger}$) at 25 °C in a series of aqueous ethanol (90%, 80% and 70%) mixtures against the calculated free energies of activation ($\Delta G^{\ddagger}$) obtained by quantum-chemical calculations for epoxidation using a polarizable continuum that mimics water as a solvent. The correlation plot in 90% aqueous ethanol is presented in Figure 3A (plots obtained for the other two solvents are shown in Figures S9 and S10 in Supporting Information). The correlation is reasonably good (r = 0.963), justifying the model used. Moreover, slopes of the plots are close to unity, indicating that the leaving groups indeed have effects on the barriers of the heterolysis reactions similar to those of the modeled heterolytic epoxy ring formations.

Our further aim was to estimate the barriers and the rate constants for solvolysis of a vast number of different benzoates in aqueous ethanol mixtures based on the above correlation and to extract the corresponding nucleofugality parameters. Good linear correlation is crucial to get accurate rate constants. We found that the correlation was better between the experimental $\Delta G^{\ddagger}$ and the calculated enthalpies of activation ($\Delta H^{\ddagger}$) at 25 °C in all solvents used (r = 0.997 vs 0.963 for 90% ethanol) whereas, importantly, the slopes of those lines were also about unity (Figure 3). This might be because enthalpies obtained by PCM calculation implicitly include contributions of solvation entropies. On the other hand, without additional corrections the entropy term included into the calculated Gibbs free energy of activation tends to be quantitatively inaccurate, mostly due to the impact of low frequencies.

The next reason for good $\Delta G^{\ddagger}_{exp}$ vs $\Delta H^{\ddagger}_{calc}$ correlation comes from essentially invariant $\Delta S^{\ddagger}$ values that benzhydryl benzoates with different Z-substituents on the benzoate moiety produce in solvolysis. Kevill demonstrated that in the ethanolysis of adamantyl arenesulfonates, the rate-determining variable is the entropy of activation ($\Delta S^{\ddagger}$), while the activation enthalpies are essentially the same for all the substrates investigated.[16] However, this is not the case here for solvolysis of benzhydryl benzoates. Most $\Delta S^{\ddagger}$ obtained for solvolysis of dianisylmethyl benzoates (Table S1) are similar in magnitude (between ca. −13 and −10 cal K^{-1} mol^{-1}, so $\Delta\Delta S^{\ddagger} \approx \pm 1$ cal K^{-1} mol^{-1}), indicating that for most cases, $\Delta H^{\ddagger}$ is the rate-determining variable. Indeed, the corresponding experimental $\Delta H^{\ddagger}$ values for solvolysis of dianisylmethyl benzoates in 90% aq ethanol correlate reasonably well with the calculated $\Delta H^{\ddagger}$ values for the model reaction (the linear plot is shown in Figure S19). However, for a few substrates, such as dianisylmethyl DNB and PNB, the experimental $\Delta S^{\ddagger}$ parameters are less negative than for others. For those very cases, experimental $\Delta H^{\ddagger}$ values also deviate in the direction to cancel out the deviations of $\Delta S^{\ddagger}$. The net effect is excellent correlation between the calculated $\Delta H^{\ddagger}$ for the model reaction and the experimental $\Delta G^{\ddagger}$. The root-mean-square error for correlated experimental $\Delta G^{\ddagger}$ using the calculated $\Delta H^{\ddagger}$ in 90% aq ethanol is 0.12 kcal/mol (vs 0.35 kcal/mol for the correlation of experimental and calculated $\Delta G^{\ddagger}$ given in Figure 3A); statistical data in other solvents are similar (footnotes in Tables 3 and S7).

The linear plot between the experimental $\Delta G^{\ddagger}$ obtained in 90% aq ethanol and the calculated $\Delta H^{\ddagger}$ for the model reaction is presented in Figure 3B (correlations for 80% and 70% aq

dx.doi.org/10.1021/jo3013308 | J. Org. Chem. 2012, 77, 8986−8998

Table 3. Calculated Activation Free Energies, Solvolysis Rate Constants for Reference Dianisylmethyl Benzoates, and Related Calculated Nucleofugalities at 25 °C

solvent	Z–benzoate	$\Delta G^{\ddagger}_{calc}$ [a]	k_{calc}/s^{-1} [b]	$k_{calc} - k_{exp}/s^{-1}$	k_{rel} [c]	N_f^{calc} [d]
90E10W[e]	H (Bz)	23.20	6.14×10^{-5}	-0.86×10^{-5} (−12%)	1.0	−4.43
	2-NO_2	20.22	9.32×10^{-3}	0.22×10^{-3} (+2%)	1.5×10^{2}	−2.14
	3-NO_2	21.41	1.25×10^{-3}	-0.28×10^{-3} (−18%)	2.0×10^{1}	−3.06
	4-NO_2 (PNB)	21.34	1.42×10^{-3}	-0.02×10^{-3} (−1%)	2.3×10^{1}	−3.00
	3,5-di-NO_2 (DNB)	19.80	1.90×10^{-2}	-0.49×10^{-2} (−21%)	3.1×10^{2}	−1.76 (−0.22)
	4-CN	21.69	7.83×10^{-4}	-2.17×10^{-4} (−22%)	1.3×10^{1}	−3.27
	2-CF_3	21.14	1.97×10^{-3}	0.18×10^{-3} (+9%)	3.2×10^{1}	−2.85
	3,5-di-Cl	21.39	1.30×10^{-3}	-0.58×10^{-3} (−31%)	2.1×10^{1}	−2.95
	2,4,6-tri-F (TFB)	19.99	1.39×10^{-2}	0.14×10^{-2} (+10%)	2.3×10^{2}	−1.90 (±0.00)
	penta-F (PFB)	18.59	1.46×10^{-1}	-0.37×10^{-1} (−20%)	2.4×10^{3}	−0.93 (−0.17)
	2-MeO	22.93	9.61×10^{-5}	0.20×10^{-5} (+2%)	1.6	−4.23
	2,4,6-tri-Me	22.71	1.41×10^{-4}	-0.54×10^{-4} (−28%)	2.3	−3.93
80E20W[f]	H (Bz)	22.75	1.30×10^{-4}	0.04×10^{-4} (+3%)	1.0	−4.09
	2-NO_2	19.90	1.60×10^{-2}	0.11×10^{-2} (+7%)	1.2×10^{2}	−1.89
	3-NO_2	21.04	2.34×10^{-3}	-0.44×10^{-3} (−16%)	1.8×10^{1}	−2.77
	4-NO_2 (PNB)	20.97	2.65×10^{-3}	-0.00×10^{-3} (±0%)	2.0×10^{1}	−2.71 (+0.07)
	3,5-di-NO_2 (DNB)	19.50	3.18×10^{-2}	-0.75×10^{-2} (−19%)	2.4×10^{2}	−1.53 (−0.10)
	4-CN	21.31	1.49×10^{-3}	-0.46×10^{-3} (−24%)	1.1×10^{1}	−2.97
	2-CF_3	20.78	3.61×10^{-3}	0.44×10^{-3} (+12%)	2.8×10^{1}	−2.57
	3,5-di-Cl	21.02	2.43×10^{-3}	-0.68×10^{-3} (−22%)	1.9×10^{1}	−2.67
	2,4,6-tri-F (TFB)	19.68	2.35×10^{-2}	0.29×10^{-2} (+12%)	1.8×10^{2}	−1.66 (+0.09)
	penta-F (PFB)	18.34	2.24×10^{-1}	-0.20×10^{-1} (−8%)	1.7×10^{3}	−0.72 (−0.04)
	2-MeO	22.50	2.00×10^{-4}	0.20×10^{-4} (+10%)	1.5	−3.89
	2,4,6-tri-Me	22.28	2.89×10^{-4}	-0.94×10^{-4} (−25%)	2.2	−3.61
70E30W[g]	H (Bz)	22.48	2.06×10^{-4}	0.25×10^{-4} (+12%)	1.0	−3.88
	2-NO_2	19.69	2.29×10^{-2}	0.11×10^{-2} (+5%)	1.1×10^{2}	−1.73
	3-NO_2	20.81	3.48×10^{-3}	-0.41×10^{-3} (−11%)	1.7×10^{1}	−2.59
	4-NO_2 (PNB)	20.73	3.93×10^{-3}	-0.45×10^{-3} (−10%)	1.9×10^{1}	−2.53
	4-CN	21.07	2.24×10^{-3}	-0.80×10^{-3} (−26%)	1.1×10^{1}	−2.79
	2-CF_3	20.55	5.33×10^{-3}	0.83×10^{-3} (+16%)	2.6×10^{1}	−2.39
	3,5-di-Cl	20.79	3.61×10^{-3}	-0.90×10^{-3} (−20%)	1.8×10^{1}	−2.49
	2,4,6-tri-F (TFB)	19.47	3.33×10^{-2}	0.47×10^{-2} (+14%)	1.6×10^{2}	−1.51 (+0.17)
	penta-F (PFB)	18.16	3.02×10^{-1}	-0.11×10^{-1} (−4%)	1.5×10^{3}	−0.58 (±0.00)
	2-MeO	22.23	3.13×10^{-4}	0.41×10^{-4} (+13%)	1.5	−3.69
	2,4,6-tri-Me	22.02	4.50×10^{-4}	-0.89×10^{-4} (−17%)	2.2	−3.42

[a] In kcal mol^{-1}; calculated from $\Delta G^{\ddagger}$ (dianisylmethyl-LG)/$\Delta H^{\ddagger}$ (2-oxyethyl-LG) correlations given in Figures 3B, S6, and S7. [b] Calculated from $\Delta G^{\ddagger}_{calc}$. Differences from experimental values are given in parentheses. [c] $k_{rel} = k_{calc}$ (X-Bz)/k_{calc} (Bz). [d] Calculated from k_{calc} and related s_f using eq 1 and the E_f value for dianisylmethyl electrofuge ($E_f = 0.00$). Applied s_f values are given in Table S6. Deviations from experimental values are given in parentheses. [e] From the correlation in Figure 3B: slope = 0.97 ± 0.02, intercept = 6.60 ± 0.33 kcal mol^{-1} ($r = 0.997$; root-mean-square error = 0.12 kcal mol^{-1}). [f] From the correlation in Figure S6: slope = 0.93 ± 0.02, intercept = 6.84 ± 0.32 kcal mol^{-1} ($r = 0.997$; rms error = 0.10 kcal mol^{-1}). [g] From the correlation in Figure S7: slope = 0.91 ± 0.02, intercept = 6.91 ± 0.36 kcal mol^{-1} ($r = 0.997$; rms error = 0.10 kcal mol^{-1}).

ethanol are given in Figures S6 and S7, respectively, in Supporting Information). From the correlation lines, we calculated the rate constants for the 12 reference dianisylmethyl benzoates in aqueous ethanol mixtures and the corresponding nucleofugality parameter for a given benzoate using eq 1, as well as the deviations from the experimental data (Table 3). Data presented in Table 3 illustrate high accuracy of the model, indicating that most deviations between the calculated and experimental rate constants for solvolysis of dianisylmethyl benzoates, as well as between corresponding calculated N_f values and the experimental N_f values, are in the limits of the experimental error. It should be emphasized that similar values for rate constants have been obtained if the rate constants (and the N_f values) have been calculated from the lines obtained by correlation of the calculated $\Delta G^{\ddagger}$ for the model reaction and the experimental $\Delta G^{\ddagger}$ (presented in Figure 3A, and for 80% and 70% ethanol presented in Figures S9 and S10, respectively, in Supporting Information), but the errors are larger (Table S7 in Supporting Information).

For comparison, some reference ground-state and corresponding TS structures have been optimized in the gas phase, and the PCM single-point calculations have been performed at the same level of theory. The results (Table S5 in the Supporting Information) show that barriers obtained by PCM single-point calculations are between 1 and 2 kcal/mol lower than those obtained by PCM optimization in all the cases. However, both corelations ($\Delta G^{\ddagger}_{exp}$ vs $\Delta G^{\ddagger}_{calc}$ and $\Delta G^{\ddagger}_{exp}$ vs $\Delta H^{\ddagger}_{calc}$) are worse if PCM single-point energies have been applied ($r = 0.973$, rms error = 0.34 kcal/mol and 0.990, rms error = 0.19 kcal/mol, respectively, in 90% aq ethanol: Figure S13), indicating that PCM optimization is advantageous for this system. Our further attempt was to optimize the above-described model epoxy ring fromation reaction using one of the hybrid meta-GGA Minnesota functionals.[17] Therefore, the same 12 reference ground-state and related transition structures

dx.doi.org/10.1021/jo3013308 | J. Org. Chem. 2012, 77, 8986–8998

have been optimized using the PCM in combination with the M06-2X functional. The barriers obtained by this functional are about 6 kcal/mol higher than those obtained by B3LYP. The M06-2X calculated barriers for the model reaction have been correlated with the experimental barriers of the solvolysis presented in Scheme 1 in 90% aqueous ethanol, as described above (Figure S14 in the Supporting Information). The correlations between the experimental barriers and those obtained with M06-2X functional (r = 0.971, rms error = 0.32 kcal/mol for both $\Delta G^{\ddagger}_{exp}$ vs $\Delta G^{\ddagger}_{calc}$ and $\Delta G^{\ddagger}_{exp}$ vs $\Delta H^{\ddagger}_{calc}$ correlations) are considerably poorer than those obtained with B3LYP functional.

Method for Estimating the Reactivity (Nucleofugality) of Other Substituted Benzoates. The linear correlations presented above between the experimental $\Delta G^{\ddagger}$ and the PCM-B3LYP calculated $\Delta H^{\ddagger}$ for the model reaction provides a method for estimating the solvolytic rate constants of any dianisylmethyl benzoate in a given aq ethanol, by optimizing ground-state and TS structures, and calculating the enthalpy of activation of the model epoxy ring closure for a given benzoate. The nucleofugalities (N_f parameters) can be calculated reasonably correctly from eq 1 taking the assumption that benzoates of similar structure have similar s_f. Comparison of the calculated N_f parameters (Table 3) with experimentally obtained ones (Table 2 and reference 4) reveals that deviations are mostly within the limits of experimental error. This approach ultimately enables semiquantitative prediction of the S_N1 solvolysis rate of any combination of benzhydryl electrofuge−benzoate simply by using eq 1.[4]

To define the reactivity of a vast number of benzoates, we further optimized the structures of 67 different 2-oxyethyl-LGs in which the substituents on the benzoate moiety have systematically been varied. Also, the transition states for all corresponding epoxy ring formation reactions via concerted C—LG bond cleavage have been located (Scheme 2). The barriers and the corresponding rates for the solvolytic displacement reactions in aqueous ethanol mixtures of 67 dianisylmethyl benzoates have been calculated from the $\Delta G^{\ddagger}$/$\Delta H^{\ddagger}$ correlations presented in Figure 3B (in 90% aq ethanol) and in Supporting Information (Figures S6 and S7 for 80% and 70% aq ethanol, respectively). The predicted absolute and relative reaction rates of various dianisylmethyl benzoates in 90%, 80%, and 70% aqueous ethanol, as well as the derived nucleofugality parameters, are given in Table S6. In summary, the nucleofugalities (experimental and calculated) are now available for the spectra of about 80 benzoates that cover reactivities of 7 orders of magnitude. The most reactive LG examined here is pentacyanobenzoate, while the least reactive is 3,4,5-triaminobenzoate (Table S6).

The suitability of the above quantum-chemical model for prediction of the reactivity of various dianisylmethyl benzoates has additionally been verified by the Hammett correlation in which the logarithms of the calculated solvolysis rate constants for **6-LG** (X = Y = MeO) in 90% aq ethanol are plotted against the sum of the Hammett σ values (Figure 4).[18] Again, a very good correlation has been obtained in all solvents (r = 0.994, root-mean-square error = 0.11 in 90% aq ethanol; correlations in 80% and 70% aq ethanol are presented in Figures S16 and S17, respectively). The fact that not only monosubstituted but also di- and trisubstituted benzoates correlate well, for which the sum of the σ values has been taken into account, indicates that the calculated substituent effects on the aromatic ring are

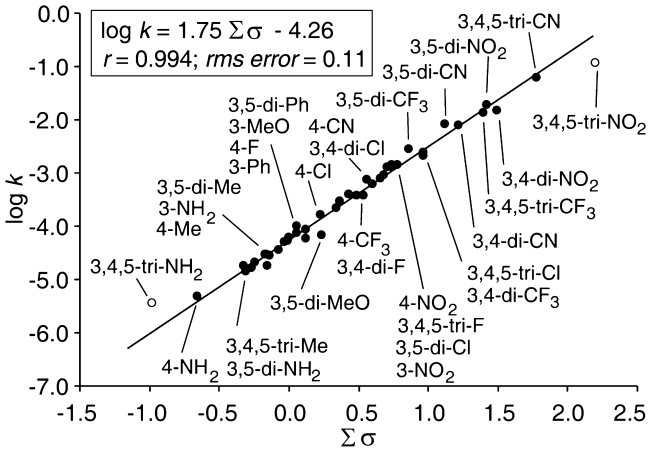

Figure 4. Hammett plot of calculated rate constants for solvolyses of dianisylmethyl benzoates in 90% ethanol at 25 °C. The deviating points represented with open circles are not included in the correlation.

additive. Therefore, the relative reactivity among the variously substituted benzoates is preserved with this model.

The Hammett ρ parameters obtained for the heterolysis reactions from the calculated rate constants are as follows: 1.75 (90% aq ethanol), 1.68 (80% aq ethanol), and 1.65 (70% aq ethanol). Those data are in accordance with the ρ values obtained earlier for heterolysis reactions that solvolyze via limited S_N1 pathway. For example, in ethanolysis of 2-adamantyl arenesulfonates and 1-adamantyl arenesulfonates the ρ parameters are 1.86 and 1.76, respectively.[16] Although for the purpose of this work only heterolytic rate constants of dianisylmethyl benzoates were used for correlations, we expect that with different benzhydryl electrofuges the quality of correlations would also be the same, which opens an even wider perspective for application of the presented model.

Intrinsic Barriers in Heterolysis of Benzoates. It is generally accepted that two major rate-determining variables are the change in reaction thermodynamics (ΔG°) and the intrinsic barrier (Λ).[19] To obtain information about how the variation of the substituents in benzoates affects the intrinsic barriers, we computed the thermoneutral methyl exchange reactions presented in Scheme 3 for 39 different benzoates,

Scheme 3. Methyl Exchange Identity Reaction

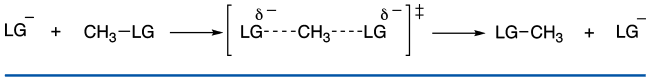

whose leaving group abilities have already been determined computationally using the above epoxy ring-formation model reaction. The calculations have also been performed at the IEFPCM-B3LYP/6-311+G(2d,p) level, taking the polarizable continuum representing water, as described in Computational Methods.

Because the thermodynamic driving force in such an identity reaction is zero, the barrier height represents the intrinsic barrier for methyl exchange, which corresponds to both intrinsic nucleofugality and intrinsic nucleophilicity of the benzoate anion. Calculated intrinsic barriers are given in Table S8.

It has repeatedly been shown for different types of reactions that the intrinsic barriers of a structurally homologous series of substrates change with variation of the structure.[20−22] In line

dx.doi.org/10.1021/jo3013308 | J. Org. Chem. 2012, 77, 8986−8998

with such observations are our results, presented in Figure 5A. The relation between the experimental barriers for solvolysis of

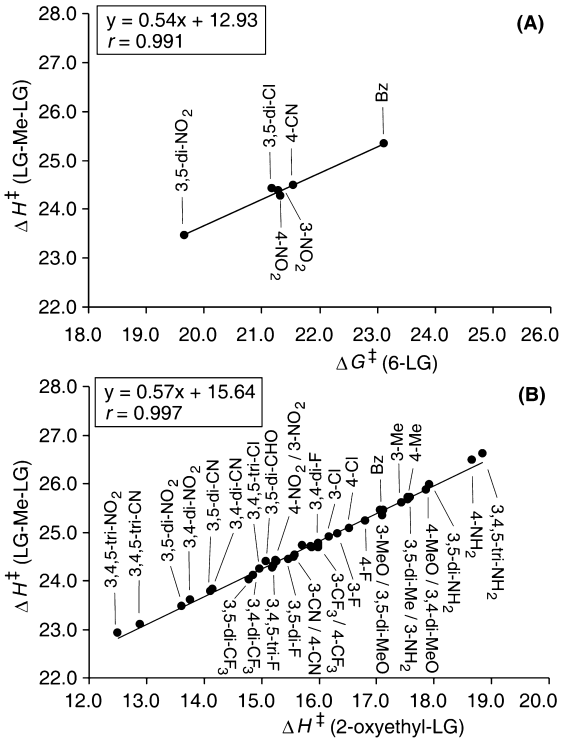

Figure 5. Correlation of calculated activation enthalpies for thermoneutral LG-Me-LG exchange versus experimental activation free energies for the solvolysis of **6**-benzoates in 90% ethanol (A), and calculated activation enthalpies for anchimerically assisted heterolytic dissociation of 2-oxyethyl benzoates (B).

dianisylmethyl derivatives and the calculated intrinsic barriers for methyl exchange (ortho-substituted benzoates are not included in the correlation because of steric and other intramolecular interactions of substituents) indicates that the intrinsic barriers increase as the overall barriers of the heterolysis increase, i.e., the intrinsic barrier is higher if a less stable benzoate leaving group is generated. Consequently, for the combination reaction (benzhydrylium ion + LG), the intrinsic barriers increase as the stability of the benzoate nucleophiles decrease.

Richard investigated numerous cases of the combination reactions of benzylic carbocations with solvents, in which the stability of carbocations varied by substituents at α-position, and demonstrated that the intrinsic barriers for the combination increased with destabilization of the carbocations caused by α-electron-withdrawing substituents, due to increasing participation of the vicinal aromatic ring electrons by resonance.[20,23] Thus, the overall barriers remain constant regardless of the changes in thermodynamic driving forces of combination reactions. The general conclusion was that the changeable Λ is due to the nonsynchronized onset of the resonance and the polar substituent effects in the TS, which has been summarized as the *Principle of nonperfect synchronization*.[21] In the case of combination reactions, the onset of the polar effects lags behind the resonance effects and, consequently, a more intense resonance effect in the TS increases the intrinsic barrier.[20a] For heterolytic reactions, an inverse order of onset of the stabilizing effects is expected. In the comprehensive kinetic study on heterolytic reactions of tritylium compounds, Mayr demonstrated unexpectedly low reactivities of dimethylamino-substituted trityl esters in comparison to methyl- and methoxy-substituted trityl esters, indicating that the amino-group stabilization of the carbocation by resonance develops noticeably later.[24]

The above premises can be used to rationalize the variable intrinsic barriers obtained with the substituted benzoates. Stabilization of the generated benzoate anion comes from the resonance on the carboxylate moiety and from the overall polar stabilization due to the electron-withdrawing substituents on the phenyl ring (field effect and inductive effect). Each electron-accepting substituent increases the polar stabilization effects of the ring but decreases the extent of the resonance effect on the carboxylate moiety in overall stabilization of TS; hence, the intrinsic barrier is successively decreased. According to the above consideration, both the thermodynamics and the intrinsic barrier influence the overall barrier for heterolysis in the same direction, the electron-withdrawing substituents stabilize the LG and also enhance the reactions by reducing the intrinsic barriers, and the electron-donating substituents on the phenyl may increase the extent of resonance on the carboxylate group and increase the intrinsic barrier. Therefore, it is not surprising that the calculated enthalpies of activation ($\Delta H^{\ddagger}$) for the model heterolytic epoxy ring formation presented in Scheme 2, and the calculated enthalpies of activation for the thermoneutral identity reaction presented in Scheme 3 correlate very well (Figure 5B).

For estimating the extent of the polar substituent effects in the TS, the normalized Hammett constant,[20a] which is here based on changes in enthalpies, has been calculated for the anchimerically assisted heterolytic dissociation of the oxyethyl-LG models (Scheme 2) according to eq 2:

$$\rho^{H}_{norm} = \frac{\rho^{H}_{activation}}{\rho^{H}_{reaction}} = \frac{-2.5}{-3.7} = 0.68 \qquad (2)$$

in which $\rho^{H}_{activation}$ represents the Hammett reaction constant obtained by plotting the calculated enthalpies of activation against the sum of corresponding Hammett σ values, whereas $\rho^{H}_{reaction}$ represents the reaction constant obtained by plotting the reaction enthalpies against the sum of σ parameters (the correlation plots are shown in Figure S18).

The substituent effects on the phenyl ring of the benzoate through polar influences are the specific rate-determining variables. According to the quantum-chemical calculations, the above fractional expression indicates that for the model reaction (Scheme 2) about 70% of substituent polar interactions are already effective in the transition states. On the other hand, calculations showed that regardless of the LG, the epoxy ring-formation model reaction (Scheme 2) is slightly exothermic (Table S4), so it proceeds via a relatively early transition state. One can speculate that if in an early TS approximately 70% of polar interactions are already operative, then the further intense stabilization after the TS must come from the resonance of the carboxylate moiety, i.e., in the heterolytic cleavage of benzoate the resonance effect lags behind the polar effects, as already concluded from the variable intrinsic barriers.

Finally, it can be concluded that the variation of the substituents on the benzoate moiety in the model reaction and in the heterolysis reaction affects $\Delta G^{\ddagger}$ by the same amount, whereas Λ values are changing proportionally to the reaction

dx.doi.org/10.1021/jo3013308 | J. Org. Chem. 2012, 77, 8986−8998

enthalpy. Combined influence of the two effects is responsible for such good correlations presented in Figure 3.

Rate Effects of the Substituents. Abundance of experimental and calculated data make it possible to examine some aspects of the influence of the phenyl ring substituents on the solvolytic reactivity of benzoates and also to find out how the solvent polarity can alter those influences.

Kevill observed that 1-adamantyl and 2-adamantyl *m*-nitrosulfonates solvolyze faster than the corresponding *p*-nitrosulfonates in ethanol, which is not in accord with the Hammett σ-parameters obtained in water ($\sigma_{p\text{-NO2}}$ = 0.78; $\sigma_{m\text{-NO2}}$ = 0.71).[16,18] Such an order of reactivity was attributed to solvent effects.

Our experimental results indicate clearly that the relative reactivities of *m*- and *p*-nitrobenzoates depend on the solvent polarity. Furthermore, we were able to detect the inversion of relative reactivities with changing solvent polarity. Thus, **6**-PNB (dianisylmethyl *p*-nitrobenzoate) solvolyzes faster in 70% aq ethanol (see entries for PNB and *m*-NO_2-Bz in Table S1), and the rates of *m*- and *p*-nitrobenzoates are almost the same in 80% ethanol, whereas in 90% the solvolysis of *m*-nitrobenzoate is faster. Similar behavior has been observed in solvolysis of anisylphenylmethyl *p*- and *m*-nitrobenzoates (**3**-PNB and **3**-*m*-NO_2-Bz; the last two entries in Table S1). Thus, *m*-nitrobenzoate is more reactive in 90% aq ethanol, whereas in 70% the rates are the same in the limits of experimental error. In summary, in more polar solvents *p*-nitrobenzoates solvolyze faster, which is consistent with Hammett σ-parameters determined in water, whereas in a less polar solvent *m*-nitrobenzoates are more reactive.

Wiberg investigated the influences of substituents on calculated gas-phase acidities of substituted benzoic acids and showed that different field effects of differently substituted phenyl rings on the carboxylate moiety are the major variables that determine the acidities, including those of *p*- and *m*-nitro groups.[25] Using Wiberg's formalism, inversion of the relative reactivities of *p*- and *m*-nitrobenzoates can be rationalized as follows: The nitro group (strong electron-withdrawing substituent) on the phenyl ring separates the charges in the phenyl ring by resonance. The partial positive charge, induced by the electron-withdrawing nitro group in para-position, comes conveniently to the vicinity of the negatively charged carboxylate group, namely to the ipso-carbon, as shown by the resonance structure **A** in Scheme 4. In *m*-nitrobenzoates the

Scheme 4

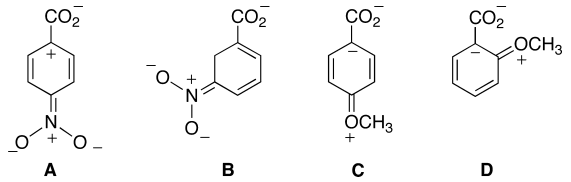

positive charge is directed to ortho-positions (structure **B**), which is of greater distance from the negatively charged carboxylate group (Scheme 4). The larger field effect slightly stabilizes the TS of *p*-nitrobenzoate over *m*-nitrobenzoate; hence, the former solvolyzes faster. However, in less polar solvents the internal charge separation in the benzoate moiety is less favored, the favorable field effect is diminished, and the greater inductivity of the meta-substituent compared with that of the para-substituent becomes the rate-determining variable causing *m*-nitrobenzoates to solvolyze faster. Therefore, in more polar solvents the distinct field effect between the para-substituted phenyl ring and the carboxylate moiety due to charge separation by resonance is the rate-determining variable, whereas in a less polar solvent it is the inductivity of the closer substituent. Because the Hammett σ-parameters have originally been determined in highly polar water, it is easy to understand why those reflect the relative reactivities of nitrobenzoates in more polar solvents. It should be mentioned that substituents on the ortho-position enhance the reaction rate significantly because of both inductive and field effects.

Using the ionizing power scale based on adamantyl tosylate, the slope parameters (m_{OTs}) of the log k vs Y_{OTs} line for dianisylmethyl *m*- and *p*-nitrobenzoates in aqueous ethanol showed that *p*-nitrobenzoates are somewhat more sensitive to solvent polarity than *m*-nitrobenzoate (m_{OTs} = 0.38 for **6**-PNB; m_{OTs} = 0.33 for **6**-3-NO_2-Bz; derived from rate constants presented in Table S1), indicating that in the transition structures the charge separation is more favored in *p*-nitrobenzoate.

To observe the substituent effects, it is useful to compare the calculated relative rate constants. In both Tables 3 and S6 the rate constant for unsubstituted dianisylmethyl benzoate is taken as a reference (k_{rel} = 1). It seems that the reaction rates obtained by calculations reflect the solvolytic behavior of the substrates in more polar solvent. For substituents whose influence on the benzoate ion stability comes from inductive effect only, as for example halogens or phenyl, the order in reactivity is ortho-substituted-Bz > meta-substituted-Bz > para-substituted-Bz. For example, according to results in Table S6, the relative reactivities of dianisyl *o*-, *m*-, and *p*-Cl-benzoates in 90% aq ethanol are: 8.2:1.8:1. However, if the charge separation in the phenyl ring is enhanced in the TS by the strong electron-withdrawing substituents, as shown above for nitrobenzoates, the calculated rates show that para-substituted benzoates solvolyze faster than meta-substituted benzoates, i.e., the more favorable inductive effect of the closer meta-substituent is canceled out with the favorable field effect of the phenyl ring with para-substituent. Similar behavior is also predicted for benzoates with strong electron-withdrawing CHO and CN groups (Table S6). Such an order of reactivities is consistent with experimental data obtained in 70% aq ethanol.

The methoxy group is the example of substituent which has a stabilizing effect by inductivity but an unfavorable destabilizing charge distribution effect by resonance (structures **C** and **D** in Scheme 4). It seems that those two effects compensate for each other in *m*-methoxybenzoate, so its calculated solvolysis rates in aqueous ethanol solutions are essentially the same as the rates of unsubstituted benzoate.

In *p*-MeO-benzoates the inductive effect on a more remoted position is less important, whereas the unfavorable repulsive field effect is enhanced by the ability of the methoxy group to distribute additional negative charge to the ipso-position, which is in the vicinity of the negatively charged carboxylate moiety (resonance structure **C** in Scheme 4). Therefore, *p*-methoxybenzoates solvolyze slower than the corresponding *m*-methoxy benzoates. However, if the methoxy group is located in ortho-position, the favorable inductive effect is strong enough to overcome the destabilizing field effect (resonance structure **D**) causing the enhancement of the rate in comparison to unsubstituted benzoate.

dx.doi.org/10.1021/jo3013308 | J. Org. Chem. 2012, 77, 8986−8998

CONCLUSION

The solvolysis of X,Y-substituted benzhydryl benzoates proceeds via an S_N1 path in which the substituents on the phenyl ring of the benzoate moiety represent a major rate-determining factor by polar effects, i.e., by field and inductive effects. The intrinsic barriers of such reactions are variable and depend on the substituents on the phenyl ring in the benzoate moiety in a way that the more stabilized LG proceeds over a lower intrinsic barrier. The experimental barriers for the solvolysis of benzhydryl benzoates and those for the heterolytic epoxy ring formation, calculated by PCM quantum-chemical calculations, correlate linearly, providing the model for extrapolation of the reactivity of any benzhydryl benzoate and also for calculation of the nucleofugality of a given benzoate in a given solvent. Using the method presented above, the theoretical nucleofugality parameters for about 70 benzoates have been determined in 90%, 80%, and 70% aqueous ethanol. Furthermore, using eq 1 and taking those nucleofugalities determined here, the heterolysis reaction for any combination of the electrofuge−benzoate nucleofuge can be determined semiquantitatively in a series of aqueous ethanol solutions.

EXPERIMENTAL SECTION

Substrate Preparation. *4-Methylbenzhydrol, 4-methoxybenzhydrol, and 4,4′-dimethoxybenzhydrol* were prepared by the reduction of the commercially available substituted benzophenones with sodium borohydride in methanol.

4-Phenoxybenzhydrol, 4-methoxy-4′-methylbenzhydrol, and 4-methoxy-4′-phenoxybenzhydrol were prepared according to the procedure given in the ref 6a.

General Procedure for the Synthesis of Benzhydryl Pentafluorobenzoates. A solution of pentafluorobenzoyl chloride (3.3 mmol) in anhydrous benzene (10 mL) was added dropwise to the previously prepared vigorously stirring solution of appropriate benzhydrol (3.0 mmol) and pyridine (6.7 mmol) in anhydrous benzene (30 mL). The reaction mixture was stirred for 12 h under an atmosphere of argon at ambient temperature. Precipitated pyridinium chloride was removed by filtration, and the excess of pyridine was removed by 10% hydrochloric acid. The benzene layer was separated and washed with water. After drying over anhydrous sodium sulfate, benzene was evaporated in vacuo to give pale-yellow oil. Recrystallization from light petroleum ether afforded white crystals (yield 59−87%).

4-Methylbenzhydryl pentafluorobenzoate: (**1-PFB**) from 4-methylbenzhydrol (0.60 g; 3.0 mmol), pyridine (0.53 g; 6.7 mmol), and pentafluorobenzoyl chloride (0.77 g; 3.3 mmol); yield 0.96 g, 81.0%; mp 91.1−91.7 °C; ^{1}H NMR (300 MHz, $CDCl_3$, 20 °C): δ = 2.33 (s, 3H; $ArCH_3$), 7.09−7.42 (m, 10H; Ar_2CH); ^{13}C NMR (75 MHz, $CDCl_3$, 20 °C): δ = 21.3 ($ArCH_3$), 79.9 (Ar_2CH), 127.2, 127.4, 128.4, 128.8, 129.5, 136.3, 138.4, 139.3 (Ar); ^{19}F NMR (282 MHz, $CDCl_3$, 20 °C): δ = −137.8, −148.5, −160.5 (F_5Ar) ppm. MALDI-TOF/TOF MS calcd for $C_{21}H_{13}F_5O_2$ [M + K^+]: 431.0467; found: 431.0486.

4-Phenoxybenzhydryl pentafluorobenzoate: (**2-PFB**) from 4-phenoxybenzhydrol (0.75 g; 2.7 mmol), pyridine (0.47 g; 6.0 mmol), and pentafluorobenzoyl chloride (0.60 g; 3.0 mmol); yield 0.80 g, 59.0%; mp 76.7−77.6 °C; ^{1}H NMR (300 MHz, $CDCl_3$, 20 °C): δ = 6.96−7.44 (m, Ar_2CH + ArH); ^{13}C NMR (75 MHz, $CDCl_3$, 20 °C): δ = 79.5 (Ar_2CH), 118.7, 119.5, 123.7, 127.1, 128.5, 128.9, 129.1, 130.0, 133.9, 139.2, 156.7, 157.8 (Ar); ^{19}F NMR (282 MHz, $CDCl_3$, 20 °C): δ = −137.7, −148.2, −160.3 (F_5Ar) ppm; elemental analysis calcd (%) for $C_{26}O_3F_5H_{15}$ (470.38): C 66.38, H 3.21; found C 66.38, H 3.00.

4-Methoxybenzhydryl pentafluorobenzoate: (**3-PFB**) from 4-methoxybenzhydrol (0.93 g; 4.3 mmol), pyridine (0.76 g; 9.6 mmol), and pentafluorobenzoyl chloride (1.10 g; 4.8 mmol); yield 1.26 g, 71.0%; mp 85.1−86.4 °C; ^{1}H NMR (300 MHz, $CDCl_3$, 20 °C): δ = 3.79 (s, 3H; $ArOCH_3$), 6.89 (d, J = 8.8 Hz, 2H; ArH), 7.09 (s, 1H; Ar_2CH), 7.30−7.42 (m, 7H; ArH); ^{13}C NMR (75 MHz, $CDCl_3$, 20 °C): δ = 55.4 ($ArOCH_3$), 79.4 (Ar_2CH), 114.2, 121.7, 127.0, 128.4, 128.8, 129.0, 139.1, 159.8 (Ar); ^{19}F NMR (282 MHz, $CDCl_3$, 20 °C): δ = −137.9, −148.5, −160.5 (F_5Ar) ppm; elemental analysis calcd (%) for $C_{21}O_3F_5H_{13}$ (408.30): C 61.77, H 3.21; found C 61.55, H 3.26.

4-Methoxy-4′-methylbenzhydryl pentafluorobenzoate: (**4-PFB**) from 4-methoxy-4′-methylbenzhydrol (1.00 g; 4.4 mmol), pyridine (0.76 g; 9.6 mmol), and pentafluorobenzoyl chloride (1.11 g; 4.8 mmol); yield 1.30 g, 71.9%; mp 114.6−116.9 °C; ^{1}H NMR (300 MHz, $CDCl_3$, 20 °C): δ = 2.34 (s, 3H; $ArCH_3$), 3.79 (s, 3H; $ArOCH_3$), 6.88 (d, J = 8.0 Hz, 2H; ArH), 7.06 (s, 1H; Ar_2CH), 7.16−7.36 (m, 6H; ArH); ^{13}C NMR (75 MHz, $CDCl_3$, 20 °C): δ = 21.3 ($ArCH_3$), 55.4 ($ArOCH_3$), 79.7 (Ar_2CH), 114.1, 127.1, 128.9, 129.5, 131.4, 136.4, 138.3, 159.6 (Ar); ^{19}F NMR (282 MHz, $CDCl_3$, 20 °C): δ = −137.9, −148.6, −160.5 (F_5Ar) ppm. MALDI-TOF/TOF MS calcd for $C_{22}H_{15}F_5O_3$ [M + Na^+]: 445.0833; found: 445.0855.

4-Methoxy-4′-phenoxybenzhydryl pentafluorobenzoate: (**5-PFB**) from 4-methoxy-4′-phenoxybenzhydrol (0.80 g; 2.6 mmol), pyridine (0.45 g; 5.7 mmol), and pentafluorobenzoyl chloride (0.66 g; 2.9 mmol); yield 1.14 g, 87.0%; mp 73.6−75.8 °C; ^{1}H NMR (300 MHz, $CDCl_3$, 20 °C): δ = 3.80 (s, 3H; $ArOCH_3$), 6.88−7.37 (m, 14H; Ar_2CH + ArH); ^{13}C NMR (75 MHz, $CDCl_3$, 20 °C): δ = 55.5 ($ArOCH_3$), 79.3 (Ar_2CH), 114.2, 118.7, 119.4, 123.8, 128.8, 130.0, 131.4, 134.0, 156.8, 157.7, 159.8 (Ar); ^{19}F NMR (282 MHz, $CDCl_3$, 20 °C): δ = −137.8, −148.4, −160.4 (F_5Ar) ppm; MALDI-TOF/TOF MS calcd for $C_{27}H_{17}F_5O_4$ [M + Na^+]: 523.0939; found: 523.0945.

4,4′-Dimethoxybenzhydryl pentafluorobenzoate: (**6-PFB**) from 4,4′-dimethoxybenzhydrol (1.00 g; 4.1 mmol), pyridine (0.71 g; 9.0 mmol), and pentafluorobenzoyl chloride (1.04 g; 4.5 mmol); yield 1.17 g, 65.0%; mp 106.7−108.5 °C; ^{1}H NMR (300 MHz, $CDCl_3$, 20 °C): δ = 3.79 (s, 6H; $ArOCH_3$), 6.89 (d, J = 8.8 Hz, 4H; ArH), 7.06 (s, 1H; Ar_2CH), 7.32 (d, J = 8.7 Hz, 4H; ArH); ^{13}C NMR (75 MHz, $CDCl_3$, 20 °C): δ = 55.4 ($ArOCH_3$), 79.5 (Ar_2CH), 114.1, 128.7, 131.4, 159.8 (Ar); ^{19}F NMR (282 MHz, $CDCl_3$, 20 °C): δ = −138.1, −148.6, −160.6 (F_5Ar) ppm; elemental analysis calcd (%) for $C_{22}O_4F_5H_{15}$ (438.34): C 60.28, H 3.45; found C 60.43, H 3.31

General Procedure for the Synthesis of Benzhydryl 2,4,6-Trifluorobenzoates. The procedure is the same as previously described for pentafluorobenzoates except that 2,4,6-trifluorobenzoyl chloride was used instead the pentafluoro analogue. 4-Phenoxy- and 4-methoxy-4′-phenoxybenzhydryl 2,4,6-trifluorobenzoate were obtained as pale yellow oils, while the others were obtained as white crystals (yield 71.2−81.1%).

4-Phenoxybenzhydryl 2,4,6-trifluorobenzoate: (**2-TFB**) from 4-phenoxybenzhydrol (0.70 g; 2.5 mmol), pyridine (0.44 g; 5.6 mmol), and trifluorobenzoyl chloride (0.54 g; 2.8 mmol); yield 0.77 g, 70.0%); ^{1}H NMR (300 MHz, $CDCl_3$, 20 °C): δ = 6.70−7.45 (Ar_2CH + ArH + F_2ArH); ^{13}C NMR (75 MHz, $CDCl_3$, 20 °C): δ = 78.3 (Ar_2CH), 101.4 (t, J = 26.2, 2C; F_3ArH), 118.7, 119.4, 123.8, 127.2, 128.3, 128.8, 129.0, 130.0, 134.4, 139.6, 156.9, 157.5 (Ar); ^{19}F NMR (282 MHz, $CDCl_3$, 20 °C): δ = −101.6, −105.5 (F_3Ar) ppm. MALDI-TOF/TOF MS calcd for $C_{26}H_{17}F_3O_3$ [M + K^+]: 473.0761; found: 473.0774.

4-Methoxybenzhydryl 2,4,6-trifluorobenzoate: (**3-TFB**) from 4-methoxybenzhydrol (0.60 g; 2.8 mmol), pyridine (0.49 g; 6.2 mmol), and trifluorobenzoyl chloride (0.60 g; 3.1 mmol); yield 0.74 g, 71.2%; mp 85.7−87.9 °C; ^{1}H NMR (300 MHz, $CDCl_3$, 20 °C): δ = 3.73 (s, 3H; $ArOCH_3$), 6.67 (t, J = 8.4 Hz, 2H; F_3ArH), 6.84 (d, J = 8.7 Hz, 2H; ArH), 7.04 (s, 1H; Ar_2CH), 7.24−7.39 (m, 7H; ArH); ^{13}C NMR (75 MHz, $CDCl_3$, 20 °C): δ = 55.4 ($ArOCH_3$), 78.6 (Ar_2CH), 101.4 (t, J = 26.2, 2C; F_3ArH), 114.1, 121.8, 127.1, 128.2, 128.7, 129.0, 131.9, 139.9, 159.6 (Ar); ^{19}F NMR (282 MHz, $CDCl_3$, 20 °C): δ = −101.9, −105.7 (F_3Ar) ppm . MALDI-TOF/TOF MS calcd for $C_{21}H_{15}F_3O_3$ [M + K^+]: 411.0605; found: 411.0623.

4-Methoxy-4′-methylbenzhydryl 2,4,6-trifluorobenzoate: (**4-TFB**) from 4-methoxy-4′-methylbenzhydrol (0.60 g; 2.6 mmol), pyridine (0.46 g; 5.8 mmol), and trifluorobenzoyl chloride (0.56 g; 2.9 mmol); yield 0.73 g, 71.6%; mp 76.8−78.8 °C; ^{1}H NMR (300 MHz, $CDCl_3$, 20 °C): δ = 2.28 (s, 3H; $ArCH_3$), 3.73 (s, 3H; $ArOCH_3$), 6.66 (t, J = 8.4 Hz, 2H; F_3ArH), 6.81 (d, J = 8.8 Hz, 2H; ArH), 7.01 (s, 1H; Ar_2CH), 7.10−7.31 (m, 6H; ArH); ^{13}C NMR (75 MHz, $CDCl_3$, 20

dx.doi.org/10.1021/jo3013308 | J. Org. Chem. 2012, 77, 8986−8998

°C): δ = 21.3 ($ArCH_3$), 55.4 ($ArOCH_3$), 78.7 (Ar_2CH), 101.3 (t, J = 26.1, 2C; F_3ArH), 114.1, 127.1, 128.9, 129.4, 132.1, 137.0, 137.9, 159.6 (Ar); ^{19}F NMR (282 MHz, $CDCl_3$, 20 °C): δ = −102.0, −105.7 (F_3Ar) ppm. MALDI-TOF/TOF MS calcd. for $C_{22}H_{17}F_3O_3$ [M + K^+]: 425.0761; Found: 425.0768.

4-Methoxy-4′-phenoxybenzhydryl 2,4,6-trifluorobenzoate: (**5-TFB**) from 4-methoxy-4′-phenoxybenzhydrol (0.70 g; 2.3 mmol), pyridine (0.40 g; 5.1 mmol), and trifluorobenzoyl chloride (0.49 g; 2.5 mmol); yield 0.86 g, 81.1%); ^1H NMR (300 MHz, $CDCl_3$, 20 °C): δ = 3.79 (s, 3H; $ArOCH_3$), 6.69 − 7.38 (m, F_3ArH + Ar_2CH + ArH); ^{13}C NMR (75 MHz, $CDCl_3$, 20 °C): δ = 55.4 ($ArOCH_3$), 78.4 (Ar_2CH), 101.4 (t, J = 26.1, 2C; F_3ArH), 114.1, 118.7, 119.4, 123.7, 128.8, 130.0, 132.0, 134.8, 157.0, 157.3, 159.5 (Ar); ^{19}F NMR (282 MHz, $CDCl_3$, 20 °C): δ = −101.7, −105.7 (F_3Ar) ppm. MALDI-TOF/TOF MS Calcd for $C_{27}H_{19}F_3O_4$ [M + H^+]: 465.1308; found: 465.1298.

4,4′-Dimethoxybenzhydryl 2,4,6-trifluorobenzoate: (**6-TFB**) from 4,4′-dimethoxybenzhydrol (0.60 g; 2.5 mmol), pyridine (0.43 g; 5.4 mmol), and trifluorobenzoyl chloride (0.53 g; 2.7 mmol); yield 0.75 g, 75.8%; mp 98.5−99.9 °C; ^1H NMR (300 MHz, $CDCl_3$, 20 °C): δ = 3.78 (s, 6H; $ArOCH_3$), 6.71 (t, J = 8.4 Hz, 2H; F_3ArH), 6.89 (d, J = 8.8 Hz, 4H; ArH), 7.05 (s, 1H; Ar_2CH), 7.34 (d, J = 8.8 Hz, 4H; ArH); ^{13}C NMR (75 MHz, $CDCl_3$, 20 °C): δ = 55.4 ($ArOCH_3$), 78.5 (Ar_2CH), 101.3 (t, J = 26.6, 2C; F_3ArH), 114.1, 128.7, 132.1, 159.5 (Ar); ^{19}F NMR (282 MHz, $CDCl_3$, 20 °C): δ = −102.1, −105.8 (F_3Ar) ppm; elemental analysis calcd (%) for $C_{22}O_4F_3H_{17}$ (402.36): C 65.67, H 4.26; found C 65.59, H 4.42.

4,4′-Dimethoxy 4-nitrobenzoate, and 4-methoxybenzhydryl 4-nitrobenzoate were prepared according to the procedure given in the ref 5a.

4,4′-Dimethoxybenzhydryl 2-Nitrobenzoate. A solution of 2-nitrobenzoyl chloride (0.53 g, 2.9 mmol) in anhydrous benzene (10 mL) was added dropwise to the previously prepared vigorously stirring solution of 4,4′-dimethoxybenzhydrol (0.50 g, 2.1 mmol) and pyridine (0.45 g, 5.7 mmol) in anhydrous benzene (30 mL). The reaction mixture was stirred overnight under an atmosphere of argon at ambient temperature. Precipitated pyridinium chloride was removed by filtration, and the excess of pyridine was removed by 10% hydrochloric acid. The benzene layer was separated and washed with water. After being dried over anhydrous sodium sulfate, the benzene was evaporated in vacuo. The crude product was dissolved in diethyl ether (30 mL), and then about 30 mL of concd aq NaOH was added. The mixture was stirred for 1 h, and then the organic layer was separated and washed with water. After being dried over anhydrous sodium sulfate, the solvent was removed in vacuo to a give pale-yellow oil (0.60 g; yield 74.5%). ^1H NMR (300 MHz, $CDCl_3$, 20 °C): δ = 3.73 (s, 6H, $ArOCH_3$), 6.84 (d, J = 8.8 Hz, 4H; ArH), 7.00 (s, 1H, Ar_2CH), 7.25 (d, J = 8.6 Hz, 4H; ArH), 7.51−7.61 (m, 2H, O_2N-ArH), 7.68 (d, J = 6.9 Hz, 1H; O_2N-ArH), 7.81 (d, J = 6.7 Hz, 1H; O_2N-ArH); ^{13}C NMR (75 MHz, $CDCl_3$, 20 °C): δ = 55.4 ($ArOCH_3$), 79.0 (Ar_2CH), 114.1, 124.0, 127.6, 128.8, 130.2, 131.7, 132.0, 132.9, 159.6 (Ar), 164.5 (C═O) ppm. MALDI-TOF/TOF MS Calcd for $C_{22}H_{19}NO_6$ [M + (e^-)]: 393.1207; found: 393.1210.

Synthesis of Other 4,4′-Dimethoxybenzhydryl Benzoates and 4-Methoxybenzhydryl 3-Nitrobenzoate. The procedure is the same as previously described for 4,4′-dimethoxybenzhydryl 2-nitrobenzoate, except that the appropriate benzoyl chloride was used. For the synthesis of 2,4,6-trimethylbenzoate, dichloromethane instead of benzene was used as a solvent. Most of products were obtained as pale-yellow oils, except for 4,4′-dimethoxybenzhydryl 4-cyanobenzoate, 4,4′-dimethoxybenzhydryl 3,5-dichlorobenzoate, and 4,4′-dimethoxybenzhydryl 2,4,6-trimethylbenzoate, which were obtained as white crystals.

4,4′-Dimethoxybenzhydryl 3-nitrobenzoate: from 4,4′-dimethoxybenzhydrol (0.50 g; 2.1 mmol), pyridine (0.47 g; 5.9 mmol), and 3-nitrobenzoyl chloride (0.54 g; 2.9 mmol); yield 0.55 g, 70.5%); ^1H NMR (300 MHz, $CDCl_3$, 20 °C): δ = 3.79 (s, 6H; $ArOCH_3$), 6.90 (d, J = 8.8 Hz, 4H; ArH), 7.10 (s, 1H; Ar_2CH), 7.35 (d, J = 8.8 Hz, 4H; ArH), 7.64 (t, J = 8.1 Hz, 1H; O_2N-ArH), 8.38−8.64 (m, 2H; O_2N-ArH), 8.91 (s, 1H; O_2N-ArH); ^{13}C NMR (75 MHz, $CDCl_3$, 20 °C): δ = 55.5 ($ArOCH_3$), 78.2 (Ar_2CH), 114,2, 124.8, 127.7, 128.7, 129.9, 132.1, 132.3, 135.6, 148.5, 159.6 (Ar), 163.8 (C═O) ppm. MALDI-TOF/TOF MS Calcd for $C_{22}H_{19}NO_6$ [M + (e^-)]: 393.1207; found: 393.1204.

4,4′-Dimethoxybenzhydryl 4-cyanobenzoate: from 4,4′-dimethoxybenzhydrol (0.50 g; 2.1 mmol), pyridine (0.47 g; 5.9 mmol), and 4-cyanobenzoyl chloride (0.49 g; 2.9 mmol); yield 0.43 g, 55.1%; mp 128.1−130.0 °C; ^1H NMR (300 MHz, $CDCl_3$, 20 °C): δ = 3.73 (s, 6H; $ArOCH_3$), 6.84 (d, J = 8.2 Hz, 4H; ArH), 7.01 (s, 1H; Ar_2CH), 7.28 (d, J = 8.7 Hz, 4H; ArH), 7.68 (d, J = 8.8 Hz, 2H; NC-ArH), 8.15 (d, J = 8.8 Hz, 2H; NC-ArH); ^{13}C NMR (75 MHz, $CDCl_3$, 20 °C): δ = 55.5 ($ArOCH_3$), 78.1 (Ar_2CH), 114.2, 116.6, 118.2, 127.9, 128.7, 130.4, 132.4, 134.4, 159.6 (Ar), 164.3 (C═O). MALDI-TOF/TOF MS calcd for $C_{23}H_{19}NO_4$ [M + (e^-)]: 373.1309; found: 373.1299.

4,4′-Dimethoxybenzhydryl 2-(trifluoromethyl)benzoate: from 4,4′-dimethoxybenzhydrol (0.50 g; 2.1 mmol), pyridine (0.47 g; 5.9 mmol), and 2-(trifluoromethyl)benzoyl chloride (0.61 g; 2.9 mmol); yield 0.69 g, 79.3%); ^1H NMR (300 MHz, $CDCl_3$, 20 °C): δ = 3.75 (s, 6H; $ArOCH_3$), 6.84 (d, J = 8.8 Hz, 4H; ArH), 7.03 (s, 1H; Ar_2CH), 7.28 (d, J = 8.8 Hz, 4H; ArH), 7.51−7.55 (m, 2H; F_3C−Ar), 7.67−7.75 (m, 2H; F_3C−Ar); ^{13}C NMR (75 MHz, $CDCl_3$, 20 °C): δ = 55.4 ($ArOCH_3$), 78.4 (Ar_2CH), 114.0, 121.7, 125.3, 126.8 (q, J = 5.4 Hz, 1C; F_3C-Ar), 127.9, 128.8, 130.4, 131.3, 131.9, 132.1, 159.5 (Ar), 165.9 (C═O); ^{19}F NMR (282 MHz, $CDCl_3$, 20 °C): δ = −59.8 (F_3C−Ar) ppm. MALDI-TOF/TOF MS Calcd for $C_{23}H_{19}F_3O_4$ [M + H^+]: 417.1308; found: 417.1304.

4,4′-Dimethoxybenzhydryl 3,5-dichlorobenzoate: from 4,4′-dimethoxybenzhydrol (0.50 g; 2.1 mmol), pyridine (0.47 g; 5.9 mmol), and 3,5-dichlorobenzoyl chloride (0.61 g; 2.9 mmol); yield 0.71 g, 80.7%; mp 91.8−93.8 °C; ^1H NMR (300 MHz, $CDCl_3$, 20 °C): δ = 3.74 (s, 6H; $ArOCH_3$), 6.85 (d, J = 8.8 Hz, 4H; ArH), 6.99 (s, 1H; Ar_2CH), 7.27 (d, J = 8.8 Hz, 4H; ArH), 7.49 (t, J = 2.0 Hz, 1H; 3,5-di-Cl-ArH), 7.91 (d, J = 2.0 Hz, 2H; 3,5-di-Cl-ArH); ^{13}C NMR (75 MHz, $CDCl_3$, 20 °C): δ = 55.5 ($ArOCH_3$), 78.1 (Ar_2CH), 114.1, 128.3, 128.7, 132.1, 133.0, 133.4, 135.5, 159.6 (Ar), 163.6 (C═O). MALDI-TOF/TOF MS Calcd for $C_{22}H_{18}Cl_2O_4$ [M + H^+]: 417.0655; found: 417.0642.

4,4′-Dimethoxybenzhydryl 2-methoxybenzoate: from 4,4′-dimethoxybenzhydrol (0.50 g; 2.1 mmol), pyridine (0.47 g; 5.9 mmol), and 2-methoxybenzoyl chloride (0.49 g; 2.9 mmol); yield 0.60 g, 75.9%); ^1H NMR (300 MHz, $CDCl_3$, 20 °C): δ = 3.73 (s, 6H; $ArOCH_3$), 3.84 (s, 3H; $ArOCH_3$), 6.83 (d, J = 8.8 Hz, 4H; ArH), 6.92 (q, J = 6.3 Hz, 2H; $ArOCH_3$), 7.00 (s, 1H; Ar_2CH), 7.32 (d, J = 8.8 Hz, 4H; ArH), 7.41 (t, J = 9.1 Hz, 1H; $ArOCH_3$), 7.84 (d, J = 8.0 Hz, 1H; $ArOCH_3$); ^{13}C NMR (75 MHz, $CDCl_3$, 20 °C): δ = 55.4 ($ArOCH_3$), 56.1 ($ArOCH_3$), 76.8 (Ar_2CH), 112.3, 114.0, 120.3, 128.0, 128.7, 132.0, 133.2, 133.8, 159.3, 159.7(Ar), 165.3 (C═O) ppm. MALDI-TOF/TOF MS Calcd for $C_{23}H_{22}O_5$ [M + K^+]: 417.1099; found: 417.1098.

4,4′-Dimethoxybenzhydryl benzoate: from 4,4′-dimethoxybenzhydrol (0.50 g; 2.1 mmol), pyridine (0.47 g; 5.9 mmol), and benzoyl chloride (0.41 g; 2.9 mmol); yield 0.49 g, 67.1%); ^1H NMR (300 MHz, $CDCl_3$, 20 °C): δ = 3.77 (s, 6H; $ArOCH_3$), 6.88 (d, J = 8.7 Hz, 4H; ArH), 7.06 (s, 1H; Ar_2CH), 7.35 (d, J = 8.3 Hz, 4H; ArH), 7.44 (t, J = 7.8 Hz, 2H; ArH), 7.55 (t, J = 7.5 Hz, 1H; ArH), 8.12 (d, J = 6.9 Hz, 2H; ArH); ^{13}C NMR (75 MHz, $CDCl_3$, 20 °C): δ = 55.5 ($ArOCH_3$), 77.0 (Ar_2CH), 114.1, 127.9, 128.7, 129.9, 130.6, 132.9, 133.2, 159.4 (Ar), 165.8 (C═O) ppm. MALDI-TOF/TOF MS calcd for $C_{22}H_{20}O_4$ [M + K^+]: 387.0993; found: 387.0975.

4,4′-Dimethoxybenzhydryl 2,4,6-trimethylbenzoate: from 4,4′-dimethoxybenzhydrol (0.50 g; 2.1 mmol), pyridine (0.47 g; 5.9 mmol), and 2,4,6-trimethylbenzoyl chloride (0.54 g; 2.9 mmol); yield 0.68 g, 82.9%; mp 71.6−73.2 °C; ^1H NMR (300 MHz, $CDCl_3$): δ = 2.12 (s, 6H; $(CH_3)_3ArH$), 2.22 (s, 3H; $(CH_3)_3ArH$), 3.74 (s, 6H; $ArOCH_3$), 6.78−6.84 (s, 2H; $(CH_3)_3ArH$ + d, J = 8.8 Hz, 4H; $ArOCH_3$), 7.06 (s, 1H; Ar_2CH), 7.29 (d, J = 8.6 Hz, 4H; ArH). ^{13}C NMR (75 MHz, $CDCl_3$): δ = 19.8, 21.3 ($(CH_3)_3ArH$), 55.4 ($ArOCH_3$), 77.1 (Ar_2CH), 114.0, 128.5, 128.9, 131.2, 132.7, 135.2, 139.4, 159.4 (Ar), 170.0 (C═O) ppm. MALDI-TOF/TOF MS calcd for $C_{25}H_{26}O_4$ [M + K^+]: 429.1462; found: 429.1474.

4-Methoxybenzhydryl 3-nitrobenzoate: from 4-methoxybenzhydrol (0.50 g; 2.3 mmol), pyridine (0.51 g; 6.4 mmol), and 3-nitrobenzoyl chloride (0.60 g; 3.2 mmol); yield 0.61 g, 72.8%); ^1H NMR (300 MHz, $CDCl_3$, 20 °C): δ = 3.79 (s, 6H; $ArOCH_3$), 6.90 (d,

dx.doi.org/10.1021/jo3013308 | J. Org. Chem. 2012, 77, 8986−8998

J = 8.8 Hz, 4H; ArH), 7.13 (s, 1H; Ar_2CH), 7.31−7.45 (m, 7H; ArH), 7.66 (t, J = 8.1 Hz, 1H; O_2N-ArH), 8.40−8.45 (m, 2H; O_2N-ArH), 8.93 (s, 1H; O_2N-ArH); ^{13}C NMR (75 MHz, $CDCl_3$, 20 °C): δ = 55.5 ($ArOCH_3$), 78.4 (Ar_2CH), 114.2, 124.8, 127.1, 127.7, 128.3, 128.8, 129.0, 129.9, 131.9, 132.2, 135.6, 139.9, 148.5, 159.7 (Ar), 163.8 (C═O) ppm. MALDI-TOF/TOF MS Calcd for $C_{21}H_{17}NO_5$ [M + K^+]: 402.0738; found: 402.0746.

Kinetic Methods. Solvolysis rate constants were measured conductometrically. Freshly prepared solvents (30 mL) were thermostatted (±0.1 °C) at a given temperature for several minutes prior to addition of the substrate. Typically, 30−60 mg of substrate was dissolved in 0.10−0.15 mL of dichloromethane and injected into the solvent. An increase of the conductivity during solvolysis was monitored automatically by means of a WTW LF 530 conductometer, using a Radiometer two-pole conductivity cell (CDC641T). Individual rate constants were obtained by least-squares fitting of the conductivity data to the first-order kinetic equation for three to four half-lives. The rate constants were averaged from at least three measurements. To achieve a complete ionization of a liberated acid, a proton sponge base [1,8-bis(dimethylamino)naphthalene] was added in a range of concentration for each given aqueous binary mixture presented in Table S3 in Supporting Information. Calibration showed the linear response of conductivity in the presented ranges of concentrations of the proton sponge base and benzoic acids liberated in examined solvolyses.

Computational Methods. All calculations were carried out using the Gaussian 09 program suit.[14] Unless otherwise noted geometry optimizations were performed without any symmetry constraints at the B3LYP/6-311+G(2d,p) level using the integral equation formalism model in a polarizable continuum (IEFPCM) representing water as solvent.[15] For charged anionic model-substrates, water has been chosen as a solvent because of its high bulk dielectric constant (ε = 78.3553). Because of solvation effects, charged systems demand additional structural relaxation in solution with respect to the gas phase. For that reason, geometry optimizations were performed by using the polarizable continuum model, which mimics a solvent, rather than in the gas phase with subsequent PCM single-point calculation. The most stable conformation found for a given ground-state structure and a conformation of the corresponding transition-state structure were used for calculation of the enthalpies of activation for both types of reactions: anchimerically assisted heterolytic dissociations of 2-oxyethyl benzoates and thermoneutral methyl exchange reactions. The transition-state structures were located using relaxed potential energy surface (PES) scans for heterolytic bond cleavage, after which the structure with the highest energy on the given PES was fully optimized. Stationary points were characterized either as minima (NImag = 0) or as saddle points (NImag = 1) by B3LYP/6-311+G(2d,p) level frequency calculations, which were also used to calculate the thermal corrections to enthalpies and free energies at 1 atm and 298 K. Values of imaginary frequencies for the anchimerically assisted heterolytic dissociation, which correspond to the oxygen attack on the α-carbon and simultaneous translation of the leaving group, vary between −550 and −560 cm^{-1} for all examined 2-oxyethyl benzoates. The imaginary frequencies for thermoneutral methyl exchange reactions are associated with the translation of the methyl group between two identical benzoate leaving groups, and their values also vary between −550 and −560 cm^{-1}. Intrinsic reaction coordinate (IRC) calculations have been employed to verify that the transition-state structures are associated with the given processes. The complexes between epoxide and benzoate leaving groups were not located despite a downward energy path with further elongation of distance between the α-carbon and leaving groups behind the TS. SCRF-PCM calculations, because of the stabilization energy of the highly polar solvent, separate ion−molecule complexes that follow the TS which results in missing the product minimum in the displacement reaction energy path.[10a] Hence, products of the heterolytic reactions were considered as free species.

The reference 2-oxyethyl benzoates and the corresponding transition-state structures were also optimized using the M06-2X functional[17] and 6-311+G(2d,p) basis set in a polarizable continuum (IEFPCM, solvent = water). Frequency calculations were performed at the same level of theory, and thermal corrections were calculated at 1 atm and 298 K. Cartesian coordinates for all optimized geometries and corresponding energies are given in the Supporting Information.

■ ASSOCIATED CONTENT

Ⓢ Supporting Information

Correlations of log k vs E_f in aq ethanol solutions and aq acetone solutions, correlations between experimental and calculated $\Delta G^{\ddagger}$ for heterolysis and $\Delta H^{\ddagger}$ for 2-oxyethyl-LG epoxydation, Hammett plots, calculated $\Delta G^{\ddagger}$ and rate constants for solvolysis of benzoates in aqueous ethanol solutions and their N_f parameters, intrinsic barriers, ^1H NMR and ^{13}C NMR spectra, optimized geometries (Cartesian coordinates), and corresponding energies for studied benzoates. This material is available free of charge via the Internet at http://pubs.acs.org.

■ AUTHOR INFORMATION

Corresponding Author

*E-mail: bdenegri@pharma.hr; kronja@pharma.hr.

Notes

The authors declare no competing financial interest.

■ ACKNOWLEDGMENTS

We gratefully acknowledge the financial support of this research by the Ministry of Science, Education and Sport of the Republic of Croatia (grant no. 006-0982933-2963). Computational resources provided by Isabella cluster (isabella.srce.hr) at Zagreb University Computing Centre (Srce) were used for this research.

■ REFERENCES

(1) (a) Bentley, T. W.; Schleyer, P. v. R. *Adv. Phys. Org. Chem.* **1977**, *14*, 1−67. (b) Bentley, T. W.; Llewellyn, G. *Prog. Phys. Org. Chem.* **1990**, *17*, 121−159. (c) Bentley, T. W.; Llewellyn, G.; Ryu, Z. H. *J. Org. Chem.* **1998**, *63*, 4654−4659. (d) Bentley, T. W.; Dau-Schmidt, J. P.; Llewellyn, G.; Mayr, H. *J. Org. Chem.* **1992**, *57*, 2387−2392. (e) Kevill, D. N. *Advances in Quantitative Structure-Property Relationships*; Charton, M., Ed.; JAI Press: Greenwich, CT, 1996; Vol. *1*, pp 81−115.

(2) (a) Brown, H. C.; Fletcher, R. S. *J. Am. Chem. Soc.* **1949**, *71*, 1845−1854. (b) Bingham, R. C.; Schleyer, P. v. R. *J. Am. Chem. Soc.* **1971**, *93*, 3189−3199. (c) Slutsky, J.; Bingham, R. C.; Schleyer, P. v. R.; Dickason, W. C.; Brown, H. C. *J. Am. Chem. Soc.* **1974**, *96*, 1969−1970.

(3) (a) Schleyer, P. v. R.; Jemmis, E. D.; Spitznagel, G. W. *J. Am. Chem. Soc.* **1985**, *107*, 6393−6394. (b) Richard, J. P.; Amyes, T. L.; Rice, D. J. *J. Am. Chem. Soc.* **1993**, *115*, 2523−2524. (c) Apeloig, Y.; Biton, R.; Abu-Freih, A. *J. Am. Chem. Soc.* **1993**, *115*, 2522−2523. (d) Kirmse, W.; Goer, B. *J. Am. Chem. Soc.* **1990**, *112*, 4556−4557.

(4) Streidl, N.; Denegri, B.; Kronja, O.; Mayr, H. *Acc. Chem. Res.* **2010**, *43*, 1537−1549.

(5) (a) Denegri, B.; Streiter, A.; Jurić, S.; Ofial, A. R.; Kronja, O.; Mayr, H. *Chem.—Eur. J.* **2006**, *12*, 1648−1656; *Chem.—Eur. J.* **2006**, *12*, 5415−5415. (b) Denegri, B.; Minegishi, S.; Kronja, O.; Mayr, H. *Angew. Chem., Int. Ed.* **2004**, *43*, 2302−2305.

(6) (a) Denegri, B.; Kronja, O. *J. Org. Chem.* **2007**, *72*, 8427−8433. (b) Denegri, B.; Kronja, O. *J. Org. Chem.* **2009**, *74*, 5927−5933. (c) Matić, M.; Denegri, B.; Kronja, O. *Eur. J. Org. Chem.* **2010**, 6019−6024. (d) Jurić, S.; Denegri, B.; Kronja, O. *J. Org. Chem.* **2010**, *75*, 3851−3854. (e) Jurić, S.; Denegri, B.; Kronja, O. *J. Phys. Org. Chem.* **2011**, *25*, 147−152.

(7) Matić, M.; Jurić, S.; Denegri, B.; Kronja, O. *Int. J. Mol. Sci.* **2012**, *13*, 2012−2024.

(8) Denegri, B.; Kronja, O. *J. Phys. Org. Chem.* **2009**, *22*, 495−503.

(9) (a) Boyd, D. B. *J. Org. Chem.* **1985**, *50*, 885−886. (b) Marshall, D. R.; Thomas, P. J.; Stirling, C. J. M. *J. Chem. Soc., Chem. Commun.* **1975**, 940−941.
(10) (a) Castejon, H.; Wiberg, K. B. *J. Am. Chem. Soc.* **1999**, *121*, 2139−2146. (b) Castejon, H.; Wiberg, K. B.; Sklenak, S.; Hinz, W. *J. Am. Chem. Soc.* **2001**, *123*, 6092−6097. (c) Martinez, A. G.; Vilar, E. T.; Barcina, J. O.; Cerero, S. D. *J. Org. Chem.* **2005**, *70*, 10238−10246. (d) Chen, X.; Regan, C. K.; Craig, S. L.; Krenske, E. H.; Houk, K. N.; Jorgensen, W. L.; Brauman, J. I. *J. Am. Chem. Soc.* **2009**, *131*, 16162−16170. (e) Yamataka, H.; Aida, M. *Chem. Phys. Lett.* **1998**, *289*, 105−109. (f) Ren, Y.; Yamataka, H. *Chem.—Eur. J.* **2007**, *13*, 677−682. (g) Melo, A.; Alfaia, A. J. I.; Reis, J. C. R.; Calado, A. R. T. *J. Phys. Chem. B* **2006**, *110* (4), 1877−1888.
(11) Aggarwal, V. K.; Harvey, J. N.; Robiette, R. *Angew. Chem., Int. Ed.* **2005**, *44*, 5468−5471.
(12) (a) Rodriquez, C. F.; Williams, I. H. *J. Chem. Soc., Perkin Trans. 2* **1997**, *4*, 959−965. (b) Malnar, I.; Jurić, S.; Vrček, V.; Gjuranović, Ž.; Mihalić, Z.; Kronja, O. *J. Org. Chem.* **2002**, *67*, 1490−1495. (c) Schreiner, P. R.; Schleyer, P. v. R.; Schaefer, H. F. *J. Org. Chem.* **1997**, *62*, 4216−4228.
(13) Wang, C.; Fu, Y.; Guo, Q.-X.; Liu, L. *Chem.—Eur. J.* **2010**, *16*, 2586−2598.
(14) Frisch, M. J.; Trucks, G. W.; Schlegel, H. B.; Scuseria, G. E.; Robb, M. A.; Cheeseman, J. R.; Scalmani, G.; Barone, V.; Mennucci, B.; Petersson, G. A.; Nakatsuji, H.; Caricato, M.; Li, X.; Hratchian, H. P.; Izmaylov, A. F.; Bloino, J.; Zheng, G.; Sonnenberg, J. L.; Hada, M.; Ehara, M.; Toyota, K.; Fukuda, R.; Hasegawa, J.; Ishida, M.; Nakajima, T.; Honda, Y.; Kitao, O.; Nakai, H.; Vreven, T.; Montgomery, J. A., Jr. ; Peralta, J. E.; Ogliaro, F.; Bearpark, M.; Heyd, J. J.; Brothers, E.; Kudin, K. N.; Staroverov, V. N.; Kobayashi, R.; Normand, J.; Raghavachari, K.; Rendell, A.; Burant, J. C.; Iyengar, S. S.; Tomasi, J.; Cossi, M.; Rega, N.; Millam, J. M.; Klene, M.; Knox, J. E.; Cross, J. B.; Bakken, V.; Adamo, C.; Jaramillo, J.; Gomperts, R.; Stratmann, R. E.; Yazyev, O.; Austin, A. J.; Cammi, R.; Pomelli, C.; Ochterski, J. W.; Martin, R. L.; Morokuma, K.; Zakrzewski, V. G.; Voth, G. A.; Salvador, P.; Dannenberg, J. J.; Dapprich, S.; Daniels, A. D.; Farkas, O.; Foresman, J. B.; Ortiz, J. V.; Cioslowski, J.; Fox, D. J. *Gaussian 09*, Revision A.02; Gaussian, Inc., Wallingford, CT, 2009.
(15) Tomasi, J.; Mennucci, B.; Cammi, R. *Chem. Rev.* **2005**, *105*, 2999−3093.
(16) Kevill, D. N.; Kolwyck, K. C.; Shold, D. M.; Kim, C. B. *J. Am. Chem. Soc.* **1973**, *95*, 6022−6027.
(17) (a) Zhao, Y.; Truhlar, D. G. *Theor. Chem. Acc.* **2008**, *120*, 215−241. (b) Zhao, Y.; Truhlar, D. G. *Acc. Chem. Res.* **2008**, *41*, 157−167.
(18) Sigma values were taken from Lowry, T. H.; Richardson, K. S. *Mechanism and Theory in Organic Chemistry*, 3rd ed.; Harper and Row Publishers: New York, 1987.
(19) Marcus, R. A. *J. Phys. Chem.* **1968**, *72*, 891−899.
(20) (a) Richard, J. P. *Tetrahedron* **1995**, *51*, 1535−1573. (b) Richard, J. P.; Amyes, T. L.; Williams, K. B. *Pure Appl. Chem.* **1998**, *70*, 2007−2014. (c) Richard, J. P.; Amyes, T. L.; Toteva, M. M. *Acc. Chem. Res.* **2001**, *34*, 981−988.
(21) (a) Bernasconi, C. F. *Adv. Phys. Org. Chem.* **1992**, *27*, 119−238. (b) Bernasconi, C. F. *Acc. Chem. Res.* **1992**, *25*, 9−16.
(22) Würthwein, E.-U.; Lang, G.; Schappele, L. H.; Mayr, H. *J. Am. Chem. Soc.* **2002**, *124*, 4084−4092.
(23) (a) Amyes, T. L.; Stevens, I. W.; Richard, J. P. *J. Org. Chem.* **1993**, *58*, 6057−6066. (b) Richard, J. P.; Amyes, T. L.; Bei, L.; Stubblefield, V. *J. Am. Chem. Soc.* **1990**, *112*, 9513−9519.
(24) (a) Horn, M.; Mayr, H. *Chem.—Eur. J.* **2010**, *16*, 7469−7477. (b) Horn, M.; Mayr, H. *Chem.—Eur. J.* **2010**, *16*, 7478−7487.
(25) Wiberg, K. B. *J. Org. Chem.* **2002**, *67*, 4787−4794.